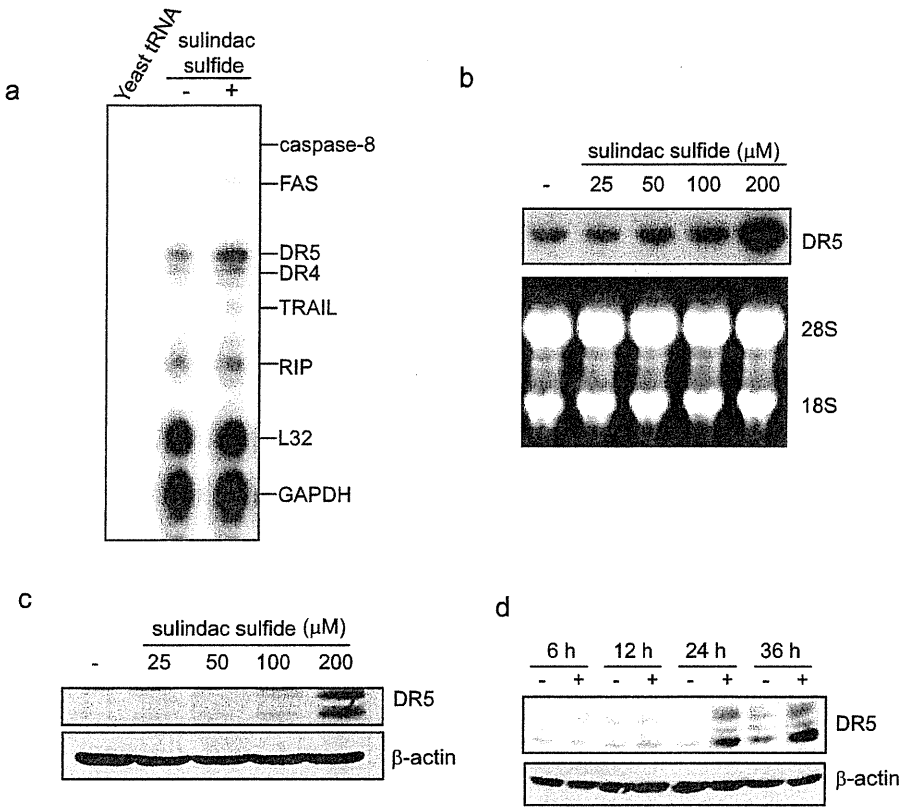

Figure 2 | Sulindac sulfide induced DR5 expression in SW480 cells. (a) RNase protection assay. SW480 cells were treated with or without 200 μM sulindac sulfide for 24 h. Total RNA from SW480 cells was hybridized with probes, and then digested with RNase as described in the Materials and Methods. The housekeeping genes GAPDH and ribosomal protein L32 are shown as controls. (b) Northern blot analysis. SW480 cells were treated with various concentrations of sulindac sulfide for 24 h. Total RNA was probed with human DR5 cDNA. Ethidium bromide staining of 28S and 18S rRNA are shown as loading controls. (c) Western blotting for DR5. SW480 cells were treated with the indicated concentrations of sulindac sulfide for 24 h. β-actin was used as a loading control. (d) Western blotting for DR5. Cells were treated with or without 200 μM sulindac sulfide for the period indicated. β-actin was used as a loading control. −, treated with solvent DMSO.

and d). Using luciferase reporter plasmids carrying the DR5 promoter, we examined the mechanism underlying how sulindac sulfide up-regulated the expression of DR5 (Fig. 3). Previous studies reported that the transcription factors p53 and NF-κB increased DR5 promoter activity through these consensus elements on intron 1[33–36]. With or without p53- and NF-κB- binding sites, DR5 promoter activity was enhanced by the sulindac sulfide treatment. These results demonstrated that sulindac sulfide up-regulated DR5 expression at a transcriptional level and the responsive element against sulindac sulfide was on the upstream promoter region of the DR5 gene.

Identification of sulindac sulfide-responsive elements in the DR5 promoter. We investigated transcription factors contributing to the upregulation of DR5 by sulindac sulfide. Using a series of deletion mutants in the DR5 promoter flanking the luciferase reporter gene, we performed luciferase assays with or without sulindac sulfide (Fig. 4). The DR5 promoter-luciferase construct pDR5/−448 as well as pDR5PF increased promoter activity by sulindac sulfide more than 2-fold, whereas the promoter activity of pDR5/−198 was not increased (Fig. 4a). This result indicates that sulindac sulfide-responsive elements are located between −448 and −199. Thus, we generated additional reporter plasmids between −448 and −199 and performed luciferase assays (Fig. 4b). Sulindac sulfide enhanced the promoter activity of pDR5/−301 more than 2-fold. On the other hand, pDR5/−252 did not respond to the sulindac sulfide treatment, which indicated that the sulindac sulfide-responsive elements of the DR5 promoter are located within a 50-bp region between −301 and −253 relative to the first base of the translation initiation codon.

We examined the predicted transcription factor-binding sites using TFSEARCH. This sequence represents the possible binding region for the transcription factor MZF1 (Fig. 5a). We introduced a site-directed mutation to the putative MZF1-binding site on the DR5 promoter and generated pDR5/mtMZF1 (Fig. 5a). As shown in Figure 5b, sulindac sulfide did not enhance the promoter activity of pDR5/mtMZF1.

Next, we examined the direct protein binding to the putative MZF1-binding site of the DR5 promoter at the condition with or without sulindac sulfide by gel shift assay. We detected the protein-DNA complex on the site and the complex was increased by sulindac sulfide treatment (Fig. 5c). Competitor oligonucleotides with an MZF1-binding sequence but not a mutant sequence strongly competed out the protein-DNA complex, indicating that the protein specifically bound to the site depending on the MZF1-binding sequence. These results indicated that sulindac sulfide up-regulated DR5 transcription via the MZF1-binding site of the DR5 promoter.

Sulindac sulfide also induced MZF1 expression and knockdown of MZF1 blocked the upregulation of DR5 by sulindac sulfide. As described above, MZF1 was suggested to contribute to the enhancement of the DR5 promoter by sulindac sulfide. We investigated the behavior of MZF1 when treated with sulindac sulfide. The expression of MZF1 was increased by the sulindac

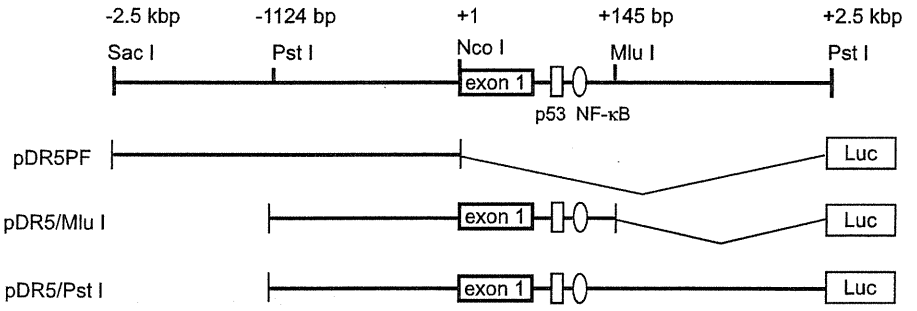

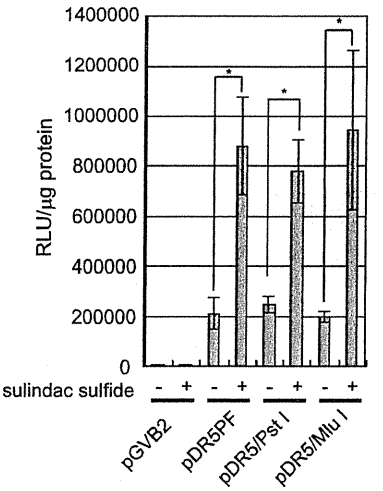

Figure 3 | Sulindac sulfide induced DR5 promoter activity in SW480 cells. SW480 cells were transiently transfected with reporter plasmids containing various sizes of DR5 promoters and the luciferase gene. Twenty-four hours after the transfection, cells were treated with or without 200 μM sulindac sulfide for 24 h, and cell lysates were the harvested for the luciferase assay, as described in the Materials and Methods. Relative luciferase activity is shown as raw light units (RLU) standardized with the protein concentrations. Data represent the means of triplicate experiments (bars, S.D.). −: treated with solvent DMSO. *: $p < 0.05$.

sulfide treatment (Fig. 6a). Thus, we examined whether MZF1 induction was related to the expression of DR5. In another human colon cancer HCT116 cells, the expressions of DR5 and MZF1 were similarly induced by sulindac sulfide (Supplemental Figure). The overexpression of MZF1 increased DR5 promoter activity, whereas the DR5 promoter with a mutation in the MZF1-binding site was not activated by the overexpression of MZF1 (Fig. 6b). We also examined the MZF1 knockdown effect on the upregulation of DR5 by sulindac sulfide. MZF1 siRNA reduced the upregulation of DR5 by sulindac sulfide (Fig. 6c), which indicated that MZF1 at least partially mediated the upregulation of DR5 induced by sulindac sulfide.

Discussion

Sulindac sulfide was previously suggested to be a candidate for a TRAIL sensitizer due to the upregulation of DR5[27]. However, the mechanism underlying how sulindac sulfide up-regulates DR5 has not yet been elucidated. In the present study, we demonstrated for the first time that MZF1, a transcription factor containing the Zinc-finger domain, mediated the sulindac sulfide-induced upregulation of DR5. Sulindac sulfide increased DR5 protein and mRNA levels as well as upstream promoter activity (Fig. 2 and 3). We identified a responsive element regulated by sulindac sulfide using a series of mutant plasmids in the DR5 promoter, and the element contained a consensus sequence of the MZF1-binding site with 100% identity (Fig. 4 and 5a, b). Next, we confirmed the direct MZF1 binding to the putative MZF1-binding site of the DR5 promoter (Fig. 5c). Furthermore, we showed the expression of MZF1 was increased by sulindac sulfide (Fig. 6a). The overexpression of MZF1 increased DR5 promoter activity through the element and knockdown of MZF1 abrogated the upregulation of DR5 by sulindac sulfide (Fig. 6b, c). These results indicate that MZF1 is a transcriptional regulator of DR5 expression and a mediator for the induction of DR5 by sulindac sulfide (Fig. 7).

Some direct transcription factors for DR5 expression have so far been reported and include p53[33,34], NF-κB[35,36], c-Myc[37], CHOP[38–40], and YY1[41]. Oncogenic stresses, such as NF-κB and c-Myc, have been shown to enhance the expression of DR5. In the present study, we also showed that MZF1, which is known to possess an oncogenic function, is a novel transcriptional regulator of DR5. The aberrant expression of MZF1 facilitates cancer cell proliferation and invasion[42,43]. In this study, we showed that sulindac sulfide increased the expression of MZF1 (Fig. 6); however, sulindac sulfide did not induce proliferation in human colon cancer SW480 cells (data not shown). The mechanism underlying the induction of MZF1 by sulindac sulfide remains unclear; however, a non-steroidal anti-inflammatory drug activated gene (NAG-1) was shown to be induced by

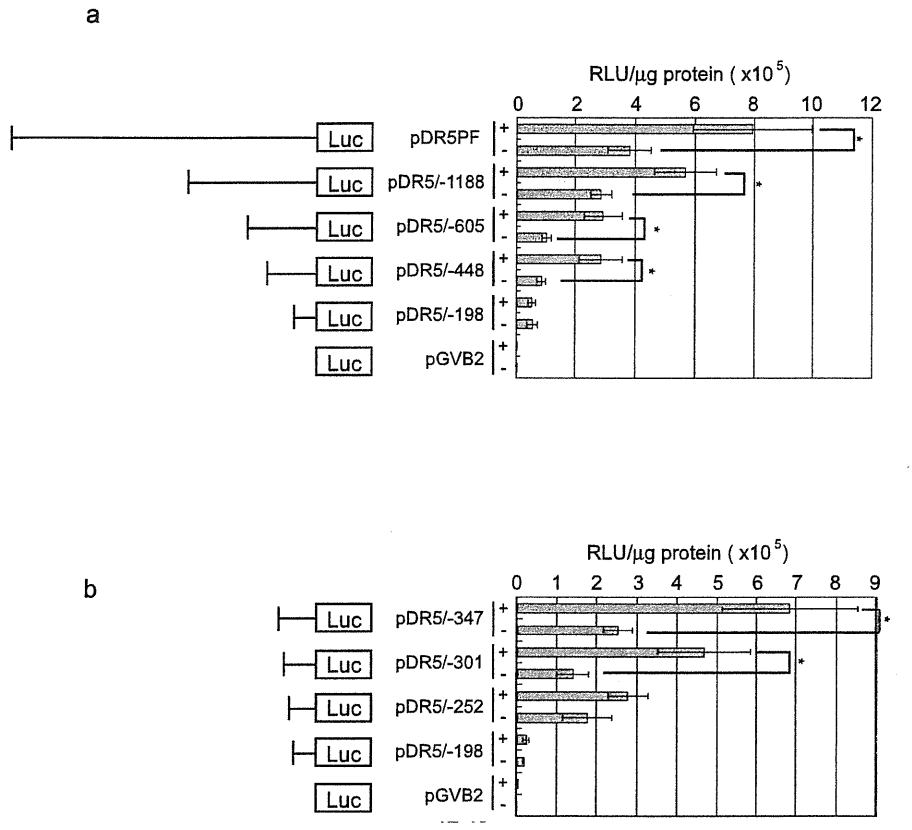

Figure 4 | Analysis of sulindac sulfide-responsive elements in the DR5 promoter. (a)(b) The luciferase assay was performed as described in Figure 3 with the indicated reporter plasmids. Data represent the means of triplicate experiments (bars, S.D.). +: treated with 200 μM sulindac sulfide for 24 h, −: treated with solvent DMSO. *: $p < 0.05$.

sulindac sulfide and correlated to the induction of DR5[44]. Therefore, we postulated that NAG-1 may be a candidate regulator for the induction of MZF1.

Sulindac sulfide induces DR5 in a tumor-suppressor p53-independent manner, and DR5 is a downstream gene of the tumor-suppressor p53[33,34]. We showed that the intronic p53-resposive site was not responsible for the activation of the promoter by sulindac sulfide (Fig. 3). Moreover, human colon cancer SW480 cells, which were mainly used in the present study, carried a mutated p53. These findings support the clinical benefit of combining sulindac sulfide and TRAIL, because more than half of malignant tumors possess inactivating mutations in the p53 gene[45,46]. Our results suggest that the combined treatment with sulindac sulfide and TRAIL is a promising strategy against tumors carrying a p53 mutation.

We proposed that sulindac sulfide can enhance TRAIL sensitivity against cancer cells. However, our results also suggested that TRAIL may enhance the chemopreventive efficacy of NSAIDs such as sulindac sulfide. Although, NSAIDs are frequently prescribed worldwide, adverse effects such as gastrointestinal bleeding are considered problematic. Based on our present results, TRAIL inducers may be candidates that can reduce the effective dose of NSAIDs. We previously reported that lactobacilli and *Clostridium butyricum* MIYAIRI 588 facilitated the production of TRAIL[47,48]. These results suggest that the combination with NSAIDs and probiotics as a TRAIL inducer may be a useful strategy for cancer chemoprevention through the TRAIL-DR5 pathway.

Methods

Reagents. Sulindac sulfide (Calbiochem, La Jolla, CA) was dissolved in DMSO. Soluble recombinant human TRAIL/Apo2L was purchased from PeproTech (London, UK). zVAD-fmk, a pan-caspase inhibitor, was purchased from R&D Systems (Minneapolis, MN).

Cell culture. Human colon cancer SW480 cells and HCT116 cells were purchased from the American Type Culture Collection (ATCC) and propagated and maintained according to protocols supplied by ATCC. Cells were cultured in Dulbecco's modified Eagle's medium supplemented with 10% fetal bovine serum, 4 mM glutamine, 100 U/ml penicillin, and 100 μg/ml streptomycin at 37°C, with humidity and 5% CO_2. Cell line authentication was not performed by the authors within the last 6 months.

Detection of apoptosis. DNA fragmentation was quantified by the percentage of hypodiploid DNA (sub-G1). Cells were treated with the agent and harvested from culture dishes. After being washed with PBS, cells were suspended in 0.1% Triton-X100/PBS solution. Cells were then treated with RNase A (Sigma, St Louis, MO) and the nuclei were stained with propidium iodide (Sigma). The DNA content was measured using FACS Calibur (Becton Dickinson, Franklin Lakes, NJ). A total of 10,000 events were collected for each experiment. Cell Quest software (Becton Dickinson) was used to analyze the data.

DAPI staining was performed out as previously described[28].

RNA analysis. Total RNA was extracted from SW480 cells using Sepasol-RNA I (Nacalai Tesque, Kyoto, Japan) according to the manufacturer's instructions. The RNase protection assay was performed using MAXI script (Ambion, Austin, TX), RPA III kit (Ambion), and hAPO3d (death receptor and death ligand) template sets (BD Biosciences PharMingen, San Jose, CA), as described previously[28].

Total RNA (10 μg) was separated with electrophoresises on a 1% agarose gel and transferred to a Biodyne B nylon membrane (Pall, Pensacola, FL). Full-length DR5 cDNA was used as a probe for Northern blot analysis. Hybridization was performed with a ^{32}P-labelled probe in PerfectHyb PLUS Hybridization buffer (Toyobo, Osaka, Japan) at 68°C for 16 h, and the membrane was washed at 68°C in 2 × SSC containing 0.1% SDS. The blot was exposed to X-ray films (Kodak, Chalon-sur-Saone, France).

Western blot analysis. Whole cell lysates were prepared as described previously[29]. The cell lysate was separated on 10% SDS-polyacrylamide gel for electrophoresis, and blotted onto polyvinylidene difluoride (PVDF) membranes (Millipore, Bedford, MA). Rabbit polyclonal antibodies for DR5 (Prosci, Poway, CA), caspase-3 (Cell Signaling Technology, Beverly, MA), and MZF1 (Santa Cruz Biotechnology, Santa Cruz, CA), and mouse monoclonal antibodies for caspase-8 (MBL, Nagoya, Japan), poly(ADP-ribose) polymerase (PARP) and β-actin (Sigma) were used as the primary antibodies. The blots were incubated with the appropriate HRP-conjugated secondary antibody (GE Healthcare, Piscataway, NJ), and signals were detected with

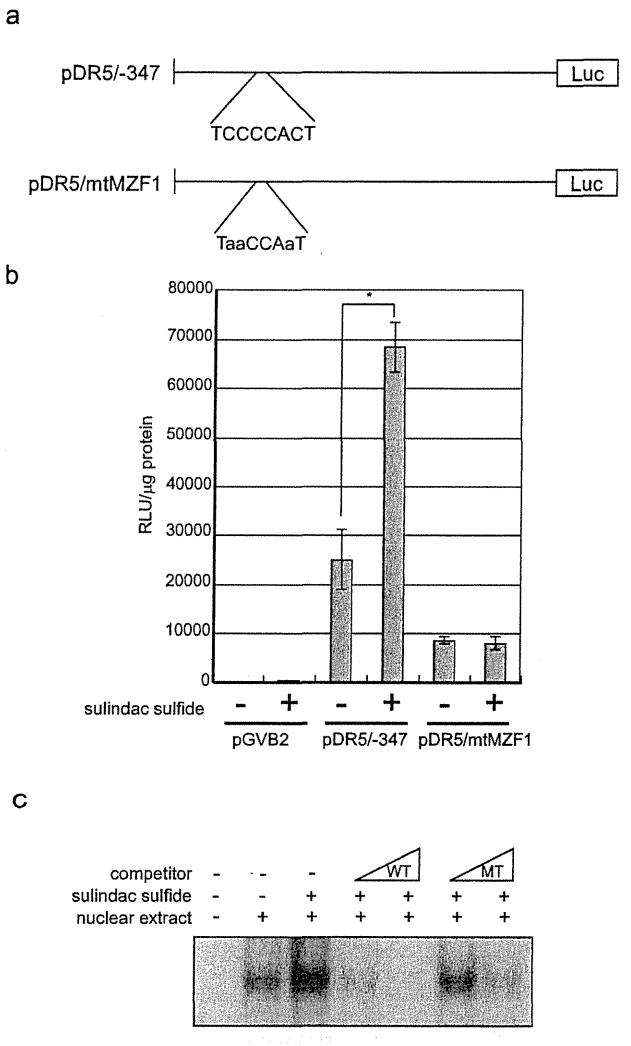

Figure 5 | Mutation in the MZF1-binding site attenuated activation of the DR5 promoter due to sulindac sulfide. (a) The sulindac sulfide-responsive region in the DR5 promoter and MZF1-binding sequences are shown. The predicted transcription factor-binding sites are shown using TFSEARCH 1.3. Mutation sequences are described in small letters. (b) The luciferase assay was performed as described in Figure 3 with the indicated reporter plasmids. Data represent the means of triplicate experiments (bars, S.D.). +: treated with 200 μM sulindac sulfide for 24 h, −: treated with solvent DMSO. *: $p < 0.05$ (c) Nuclear extract from cells treated with sulindac sulfide or DMSO were analyzed by gel shift assay, as described in Materials and methods. Increased amounts of the unlabeled oligonucleotides (×2 or ×8) were used as competitors. WT: wild-type MZF1-binding site of DR5 promoter. MT: mutant MZF1-binding site of DR5 promoter.

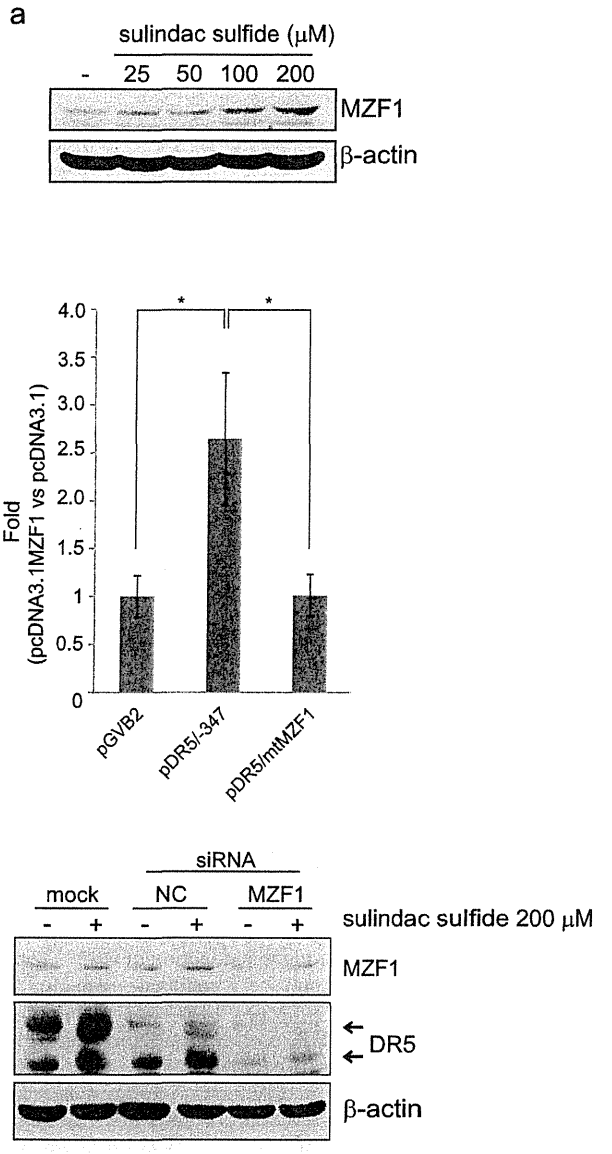

Figure 6 | Sulindac sulfide induced MZF1 expression, and MZF1 siRNA reduced the enhancement in DR5 expression by sulindac sulfide. (a) Western blotting for MZF1. SW480 cells were treated with the indicated concentrations of sulindac sulfide for 24 h. β-actin was used as a loading control. (b) The luciferase assay was performed as described in Figure 5 with the indicated reporter plasmids. The MZF1 overexpression plasmid pcDNA3.1MZF1 was co-transfected with luciferase reporter plasmids as described in the Materials and Methods. The fold induction in promoter activity (pcDNA3.1MZF1 vs control vector pcDNA3.1) was shown as a bar graph. Data represent the means +/− S.D. of three determinations. *: $p < 0.05$ (c) Western blotting for DR5 and MZF1. SW480 cells were transfected with MZF1 siRNA or negative control siRNA at 80 nM. Twenty-four hours after the transfection, cells were treated with or without 200 μM sulindac sulfide for 24 h. β-actin was used as a loading control. −: treated with DMSO, mock: transfection was performed without any siRNA.

Chemilumi-One (Nacalai Tesque) and an ECL Western blot analysis system (GE Healthcare).

DNA transfection and luciferase assay. As previously described[30–32], a digested *SacI-NcoI* fragment from the DR5 promoter region of human genomic DNA was subcloned into the *SacI-NcoI* site of the pGVB2 luciferase assay vector (Toyo Ink, Tokyo, Japan) to produce pDR5PF. 5′-deletion mutants were generated with a Mungbean-Exonuclease III system from the Kilo-sequence Deletion Kit (Takara, Tokyo, Japan). pDR5/mtMZF1 was generated with a site-directed mutagenesis kit (Stratagene, La Jolla, CA) using synthesized oligonucleotides (5′-cgcttgcggagga-ggtagttgacgagac, and 5′-agagtctcgtcaactacctcctccgc). SW480 cells (1×10^5 cells) were seeded on 6-well plates, and 1.0 μg of plasmids were transfected with the DEAE-dextran method using a CellPhect transfection kit (GE Healthcare). After 24 h incubation, cells were treated with sulindac sulfide or solvent DMSO. Twenty-four hours after the treatment with the agent, cells were collected for the luciferase assay.

The luciferase activities of cell lysates were measured with a PicaGene luciferase assay system (Toyo Ink) and normalized for the amount of protein in the cell lysate, which was measured with the Bio-Rad protein assay kit (Bio-Rad Laboratories, Hercules, CA).

To overexpress MZF1, MZF1 cDNA was subcloned into a pcDNA3.1 mammalian expression vector (Invitrogen, Carlsbad, CA) and termed as pcDNA3.1 MZF1. In brief, 1 day prior to transfection, SW480 cells were seeded in a 6-cm dish without antibiotics at a density of 80%. Plasmid DNA (8 μg) was transfected into cells using

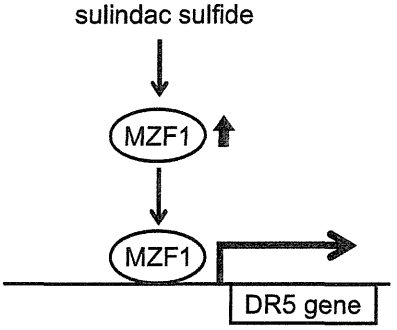

Figure 7 | The scheme of mechanisms enhancing DR5 expression by sulindac sulfide. Sulindac sulfide increases MZF1. The transcription factor MZF1 then upregulates DR5 promoter activity through its binding site.

Lipofectamine2000 reagent (Invitrogen) according to the manufacturer's instructions.

siRNA. Knockdown of MZF1 was achieved by transfection with small interfering RNA (siRNA) (Ambion) using Lipofectamine RNAiMAX (Invitrogen) according to the manufacturer's instructions.

Gel shift assay. Nuclear extracts were prepared from SW480 cells treated with DMSO or 200 μM sulindac sulfide for 12 h. The cells were lysed in buffer containing 10 mM HEPES-KOH (pH7.8), 10 mM KCl, 0.1 mM EDTA, 0.1% NP-40, 1 mM DTT, 0.5 mM PMSF, 2 μg/ml aprotinin and 2 μg/ml leupeptin, and the lysate was precipitated. The pellets were re-suspended with 50 mM HEPES-KOH (pH7.8), 420 mM KCl, 0.1 mM EDTA, 5 mM $MgCl_2$, 20% glycerol, 1 mM DTT, 0.5 mM PMSF, 2 μg/ml aprotinin and 2 μg/ml leupeptin, rotated for 30 min at 4°C and precipitated. The supernatant was used as a nuclear extract after dialysis in reaction buffer as described below. Double-stranded DNA probes containing synthetic oligonucleotides (5′-cgcgtctccccacttggaa, and 5′-gatcttccaagtggggaga) were labeled with [α-^{32}P] dCTP and Klenow. The reaction mixture contained 10 mM Tris-HCl (pH8.0), 50 mM NaCl, 2 mM $MgCl_2$, 0.5 mM EDTA, 4% glycerol, 25 μg/ml poly dI-dC, 300 μg/ml bovine serum albumin, 10 μg nuclear extracts and ^{32}P-labeled probe (50,000 cpm). The reaction mixture was incubated on ice for 20 min and resolved on 6% polyacrylamide gel in 0.25 × TBE buffer in a cold room. After electrophoresis, the gels were dried and autoradiographed at −80°C. Cold double-stranded nucleotides (wild-type: 5′-cgcgtctccccacttggaa, and 5′-gatcttccaagtggggaga, mutant: 5′-cgcgtctaaccaattggaa, and 5′-gatcttccaattggttaga) were pre-incubated with the nuclear extracts for 10 min on ice before the addition of the radiolabeled probes.

Statistical analysis. Measurements were repeated three times and statistically analyzed using a two-tailed, paired Student's *t*-test. A significant difference was determined at $p < 0.05$.

Equipment and settings. For image acquisition, all data were scanned on a Fuji Xerox DocuCentre IV C3370, multifunction printer. Scanned pictures were rotated slightly using Adobe Photoshop software.

1. Wiley, S. R. *et al.* Identification and characterization of a new member of the TNF family that induces apoptosis. *Immunity* **3**, 673–682 (1995).
2. Pitti, R. M. *et al.* Induction of apoptosis by Apo-2 ligand, a new member of the tumor necrosis factor cytokine family. *J. Biol. Chem.* **271**, 12687–12690 (1996).
3. Srivastava, R. K. TRAIL/Apo-2L: Mechanisms and clinical applications in cancer. *Neoplasia* **3**, 535–546 (2001).
4. Takeda, K. *et al.* Critical role for tumor necrosis facter-related apoptosis-inducing ligand in immune surveillance against tumor development. *J. Exp. Med.* **195**, 161–169 (2002).
5. Zerafa, N. *et al.* Cutting edge: TRAIL deficiency accelerates hematological malignancies. *J. Immunol.* **175**, 5586–5590 (2005).
6. Walczak, H. *et al.* Tumoricidal activity of tumor necrosis factor-related apoptosis-inducing ligand *in vivo*. *Nat. Med.* **5**, 157–163 (1999).
7. Ashkenazi, A. *et al.* Safety and antitumor activity of recombinant soluble Apo2 ligand. *J. Clin. Invest.* **104**, 155–162 (1999).
8. Lawrence, D. *et al.* Differential hepatocyte toxicity of recombinant Apo2L/TRAIL versions. *Nat. Med.* **7**, 383–385 (2001).
9. Ashkenazi, A., Holland, P. & Eckhardt, S. G. Ligand-based targeting of apoptosis in cancer: the potential of recombinant human apoptosis ligand 2/tumor necrosis factor-related apoptosis-inducing ligand (rhApo2L/TRAIL). *J. Clin. Oncol.* **26**, 3621–3630 (2008).
10. Johnstone, R. W., Frew, A. J. & Smyth, M. J. The TRAIL apoptotic pathway in cancer onset, progression and therapy. *Nat. Rev. Cancer* **8**, 782–798 (2008).
11. Zhang, L. & Fang, B. Mechanisms of resistance to TRAIL-induced apoptosis in cancer. *Cancer Gene Ther.* **12**, 228–237 (2005).
12. MacFarlane, M. *et al.* Identification and molecular cloning of two novel receptors for the cytotoxic ligand TRAIL. *J. Biol. Chem.* **272**, 25417–25420 (1997).
13. Pan, G. *et al.* An antagonist decoy receptor and a death domain-containing receptor for TRAIL. *Science* **277**, 815–818 (1997).
14. Sheridan, J. P. *et al.* Control of TRAIL-induced apoptosis by a family of signaling and decoy receptors. *Science* **277**, 818–821 (1997).
15. Screaton, G. R. *et al.* TRICK2, a new alternatively spliced receptor that transduces the cytotoxic signal from TRAIL. *Curr. Biol.* **7**, 693–696 (1997).
16. Walczak, H. *et al.* TRAIL-R2: a novel apoptosis-mediating receptor for TRAIL. *EMBO J.* **16**, 5386–5397 (1997).
17. LeBlanc, H. N. & Ashkenazi, A. Apo2L/TRAIL and its death and decoy receptors. *Cell Death Differ.* **10**, 66–75 (2003).
18. Horinaka, M. *et al.* Aclarubicin enhances tumor necrosis factor-related apoptosis-inducing ligand-induced apoptosis through death receptor 5 upregulation. *Cancer Sci.* **103**, 282–287 (2012).
19. Yoshida, T., Horinaka, M. & Sakai, T. Combination-oriented molecular-targeting prevention" of cancer: a model involving the combination of TRAIL and a DR5 inducer. *Environ. Health Prev. Med.* **15**, 203–210 (2010).
20. Huls, G., Koornstra, J. J. & Kleibeuker, J. H. Non-steroidal anti-inflammatory drugs and molecular carcinogenesis of colorectal carcinomas. *Lancet* **362**, 230–232 (2003).
21. Chan, A. T., Ogino, S. & Fuchs, C. S. Aspirin and the risk of colorectal cancer in relation to the expression of COX-2. *N. Engl. J. Med.* **356**, 2131–2142 (2007).
22. Rothwell, P. M. *et al.* Effect of daily aspirin on long-term risk of death due to cancer: analysis of individual patient data from randomised trials. *Lancet* **377**, 31–41 (2011).
23. Rothwell, P. M. *et al.* Effect of daily aspirin on risk of cancer metastasis: a study of incident cancers during randomised controlled trials. *Lancet* **379**, 1591–1601 (2012).
24. Chiou, S. K. & Hoa, N. Up-regulation of GADD45α expression by NSAIDs leads to apoptotic and necrotic colon cancer cell deaths. *Apoptosis* **14**, 1341–1351 (2009).
25. Tinsley, H. N. *et al.* Sulindac sulfide selectively inhibits growth and induces apoptosis of human breast tumor cells by phosphodiesterase 5 inhibition, elevation of cyclic GMP, and activation of protein kinase G. *Mol. Cancer Ther.* **8**, 3331–3340 (2009).
26. He, Q., Luo, X., Huang, Y. & Sheikh, M. S. Apo2L/TRAIL differentially modulates the apoptotic effects of sulindac and a COX-2 selective non-steroidal anti-inflammatory agent in Bax-deficient cells. *Oncogene* **21**, 6032–6040 (2002).
27. Huang, Y., He, Q., Hillman, M. J., Rong, R. & Sheikh, M. S. Sulindac sulfide-induced apoptosis involves death receptor 5 and the caspase 8-dependent pathway in human colon and prostate cancer cells. *Cancer Res.* **61**, 6918–6924 (2001).
28. Horinaka, M. *et al.* The dietary flavonoid apigenin sensitizes malignant tumor cells to tumor necrosis factor-related apoptosis-inducing ligand. *Mol. Cancer Ther.* **5**, 945–951 (2006).
29. Nakata, S. *et al.* Histone deacetylase inhibitors up-regulate death receptor 5/TRAIL-R2, and sensitize apoptosis induced by TRAIL/APO2-L in human malignant tumor cells. *Oncogene* **23**, 6261–6271 (2004).
30. Yoshida, T., Maeda, A., Tani, N. & Sakai, T. Promoter structure and transcription initiation sites of the human death receptor 5/TRAIL-R2 gene. *FEBS Lett.* **507**, 381–385 (2001).
31. Yoshida, T. & Sakai, T. Promoter of TRAIL-R2 gene. *Vitam. Horm.* **67**, 35–49 (2004).
32. Shiraishi, T. *et al.* Tunicamycin enhances tumor necrosis factor-related apoptosis-inducing ligand-induced apoptosis in human prostate cancer cells. *Cancer Res.* **65**, 6364–6370 (2005).
33. Wu, G. S. *et al.* KILLER/DR5 is a DNA damage-inducible p53-regulated death receptor gene. *Nat. Genet.* **17**, 141–143 (1997).
34. Takimoto, R. & El-Deiry, W. S. Wild-type p53 transactivates the KILLER/DR5 gene through an intronic sequence-specific DNA-binding site. *Oncogene* **19**, 1735–1743 (2000).
35. Shetty, S. *et al.* Transcription factor NF-κB differentially regulates death receptor 5 expression involving histone deacetylase 1. *Mol. Cell Biol.* **25**, 5404–5416 (2005).
36. Ravi, R. *et al.* Regulation of death receptor expression and TRAIL/Apo2L-induced apoptosis by NF-κB. *Nat. Cell Biol.* **3**, 409–416 (2001).
37. Wang, Y. *et al.* Synthetic lethal targeting of MYC by activation of the DR5 death receptor pathway. *Cancer Cell* **5**, 501–512 (2004).
38. Yamaguchi, H. & Wang, H. G. CHOP is involved in endoplasmic reticulum stress-induced apoptosis by enhancing DR5 expression in human carcinoma cells. *J. Biol. Chem.* **279**, 45495–45502 (2004).
39. Yoshida, T. *et al.* Proteasome inhibitor MG132 induces death receptor 5 through CCAAT/enhancer-binding protein homologous protein. *Cancer Res.* **65**, 5662–5667 (2005).
40. Taniguchi, H. *et al.* Baicalein overcomes tumor necrosis factor-related apoptosis-inducing ligand resistance via two different cell-specific pathways in cancer cells but not in normal cells. *Cancer Res.* **68**, 8918–8927 (2008).
41. Baritaki, S. *et al.* Regulation of tumor cell sensitivity to TRAIL-induced apoptosis by the metastatic suppressor Raf kinase inhibitor protein via Yin Yang 1 inhibition and death receptor 5 up-regulation. *J. Immunol.* **179**, 5441–5453 (2007).
42. Hromas, R. *et al.* Aberrant expression of the myeloid zinc finger gene, MZF-1, is oncogenic. *Cancer Res.* **55**, 3610–3614 (1995).

43. Gaboli, M. *et al.* Mzf1 controls cell proliferation and tumorigenesis. *Genes Dev.* **15**, 1625–1630 (2001).
44. Jang, T. J., Kang, H. J., Kim, J. R. & Yang, C. H. Non-steroidal anti-inflammatory drug activated gene (NAG-1) expression is closely related to death receptor-4 and -5 induction, which may explain sulindac sulfide induced gastric cancer cell apoptosis. *Carcinogenesis* **25**, 1853–1858 (2004).
45. Greenblatt, M. S., Bennett, W. P., Hollstein, M. & Harris, C. C. Mutations in the p53 tumor suppressor gene: clues to cancer etiology and molecular pathogenesis. *Cancer Res.* **54**, 4855–4878 (1994).
46. Levine, A. J. p53, the cellular gatekeeper for growth and division. *Cell* **88**, 323–331 (1997).
47. Horinaka, M. *et al.* Lactobacillus strains induce TRAIL production and facilitate natural killer activity against cancer cells. *FEBS Lett.* **584**, 577–582 (2010).
48. Shinnoh, M. *et al.* Clostridium butyricum MIYAIRI588 shows antitumor effects by enhancing the release of TRAIL from neutrophils through MMP-8. *Int. J. Oncol.* **42**, 903–911 (2013).

Acknowledgments

This work was partly supported by the Ministry of Education, Culture, Sports, Science and Technology of Japan.

Author contributions

T.S., M.H. and T.Y. designed the research and wrote the manuscript. M.H. and T.Y. performed the majority of the experiments. M.T., S.Y. and Y.S. supported several experiments. All authors reviewed the manuscript.

Additional information

Supplementary information accompanies this paper at http://www.nature.com/scientificreports

Competing financial interests: The authors declare no competing financial interests.

How to cite this article: Horinaka, M. *et al.* Myeloid zinc finger 1 mediates sulindac sulfide-induced upregulation of death receptor 5 of human colon cancer cells. *Sci. Rep.* 4, 6000; DOI:10.1038/srep06000 (2014).

Toxicology Reports 1 (2014) 69–73

Contents lists available at ScienceDirect

Toxicology Reports

journal homepage: www.elsevier.com/locate/toxrep

A novel aromatic mutagen, 5-amino-6-hydroxy-8*H*-benzo[6,7]azepino[5,4,3-*de*]quinolin-7-one (ABAQ), induces colonic preneoplastic lesions in mice

Takahiro Kochi[a], Masahito Shimizu[a,*], Yukari Totsuka[b], Yohei Shirakami[a], Takayuki Nakanishi[a], Tetsushi Watanabe[c], Takuji Tanaka[d], Hitoshi Nakagama[b], Keiji Wakabayashi[e], Hisataka Moriwaki[a]

[a] *Department of Internal Medicine/Gastroenterology, Gifu University Graduate School of Medicine, 1-1 Yanagido, Gifu 501-1194, Japan*
[b] *Division of Cancer Development System, National Cancer Center Research Institute, 1-1 Tsukiji 5-chome, Chuo-ku, Tokyo 104-0045, Japan*
[c] *Department of Public Health, Kyoto Pharmaceutical University, 1 Shichono-cho, Misasagi, Yamashina-ku, Kyoto 607-8412, Japan*
[d] *Department of Tumor Pathology, Gifu University Graduate School of Medicine, 1-1 Yanagido, Gifu 501-1194, Japan*
[e] *Division of Nutritional and Environmental Sciences, Institute for Environmental Sciences, University of Shizuoka, 52-1 Yada, Suruga-ku, Shizuoka 422-8526, Japan*

ARTICLE INFO

Article history:
Received 21 February 2014
Received in revised form 17 April 2014
Accepted 19 April 2014
Available online 30 April 2014

Keywords:
Benzoazepinoqunolinone
Heterocyclic amines
Maillard reaction
Fenton reaction
High-grade dysplasia
PDCD4
Colon
Dextran sodium sulfate
Initiation
Mice

ABSTRACT

The benzoazepinoqunolinone derivative, 5-amino-6-hydroxy-8*H*-benzo[6,7]azepino-[5,4,3-*de*]quinolin-7-one (ABAQ), which is produced in a mixture of glucose and tryptophan incubated at 37 °C under physiological conditions in the presence or absence of hydroxyl radicals caused by the Fenton reaction, is a novel aromatic mutagen. In the current study, we determined the tumor-initiating potency of ABAQ using an inflammation-relate, two-stage mouse colon carcinogenesis model. Male Crj: CD-1 (ICR) mice were treated with the single intragastric administration (100 or 200 mg/kg body weight) of ABAQ followed by subsequent 1-week oral exposure to 2% dextran sodium sulfate (DSS) in drinking water. The ABAQ treatment alone resulted in high-grade dysplasia, which is a precursor to colorectal cancer, in the colon. Following the administration of DSS after ABAQ treatment, the incidence and frequency of high-grade dysplastic lesions increased; the values were highest in the mice treated with 200 mg/kg body weight of ABAQ followed by DSS. The lesions expressing β-catenin in their nuclei and cytoplasm exhibited high proliferation activity without the expression of programmed cell death 4. These findings indicate that ABAQ has a tumor-initiating activity in the mouse colon, with or without inflammation, although the potential pro-inflammatory effect of high doses of ABAC should be investigated.

Abbreviations: ABAQ, 5-amino-6-hydroxy-8*H*-benzo[6,7]azepino[5,4,3-*de*]quinolin-7-one; AOM, azoxymethane; DSS, dextran sodium sulfate; HCA, heterocyclic amine; H&E, hematoxylin and eosin; i.g., intragastric; MeIQx, 2-amino-3,8-dimethylimidazo[4,5-*f*]quinoxaline; PAH, polycyclic aromatic hydrocarbons; PhIP, 2-amino-1-methyl-6-phenylimidazo[4,5-*b*]pyridine.

* Corresponding author. Tel.: +81 582306308; fax: +81 58 230 6310.
E-mail address: shimim-gif@umin.ac.jp (M. Shimizu).

http://dx.doi.org/10.1016/j.toxrep.2014.04.006

1. Introduction

Human people are continuously exogenously exposed to a variety of chemicals that have been shown to have mutagenic or carcinogenic properties in experimental systems [1]. Cooking meat and fish at a high temperature (above 180 °C) forms mutagenic and carcinogenic heterocyclic amines (HCAs) and polycyclic aromatic hydrocarbons (PAHs). HCAs are formed by the pyrolysis of creati(ni)ne with sugars with specific amino acids. Since a high temperature is needed, only fried, broiled or barbecued meat contains a significant amount of HCAs [2]. Experimental studies of HCAs began with Dr. Sugimura's discovery that cooked meat and fish contain potent mutagens [2]. Some HCAs were later shown to be complete carcinogens that induce liver, colon, mammary and prostate tumors in rodents and monkeys [2,3]. Certain HCAs are consistently identified in well-done meat products consumed in the North American diet. Although a causal link has not been fully established, a majority of epidemiology studies have linked the consumption of well-done meat products to cancer of the colon and breast. Several HCAs thus represent an important class of carcinogens in foods and have been classified as "possibly carcinogenic to humans (Group 2B)" or "probably carcinogenic to humans (Group 2A)" by the IARC [4] and "Group 2: reasonably anticipated to be human carcinogens (R)" by the NTP [5]. Similar to most other chemical carcinogens, HCAs must be metabolized by CYP1A2 or CYP1B1 to chemically reactive electrophiles prior to reacting with DNA in order to exert their carcinogenic potency in both rats and humans [2].

Certain compounds that are mutagenic and carcinogenic in cooked foods are formed by the Maillard reaction of reducing sugars and amino acids. Indeed, 2-amino-3,8-dimethylimidazo[4,5-*f*]quinoxaline (MeIQx) and 2-amino-1-methyl-6-phenylimidazo[4,5-*b*]pyridine (PhIP) are mutagenic and carcinogenic HCAs formed through the Maillard reaction in meat and fish cooked at a high temperature [2]. These compounds are suggested to be formed by the reaction of creatine with Maillard reaction products from glucose and amino acids by heating at a high temperature of 128 °C [2,3,6]. The Maillard reaction can also occur at physiological temperatures. In a series of our study performed to clarify the formation of mutagens during the Maillard reaction in glucose and amino acids, we recently identified a novel aromatic mutagen, 5-amino-6-hydroxy-8*H*-benzo[6,7]azepino[5,4,3-*de*]quinolin-7-one (ABAQ, $C_{16}H_{11}N_3O_2$, MW = 277.28, Fig. 1a), formed in the mixture of glucose and tryptophan incubated at 37 °C and a pH of 7.4 in the presence or absence of hydroxyl radicals produced by the Fenton reaction [7]. ABAQ exhibits a strong mutagenic activity toward *S. typhimurium* TA98 and YG1024 with S9 mix [7]. The mutagenic potency of ABAQ is comparable to that of PhIP [7]. ABAQ also revealed mutagenicity in the liver of *gpt* delta transgenic mice [8].

In order to understand the effects of ABAQ on human health, it is important to elucidate its tumor-initiating ability in rodents. The current study thus aimed to determine whether the novel mutagen ABAQ possesses a tumor-initiation activity in the colon in *in vivo* experiment in mice. We used an experimental model employing a colitis-inducing agent, dextran sodium sulfate (DSS), which has a powerful tumor-promotion activity [9], since the tumor-initiation activity of PhIP [10] and aminophenylnorharman [11] can be detected within a short-term period in this model. The single administration with ABAQ in two doses *via* gavage resulted in development of high-grade dysplasia in the inflamed colon induced by DSS in male mice. The immunohistochemical analysis revealed the lesions with a high proliferative activity and cytoplasmic and/or nuclear expression of β-catenin to be negative for programmed cell death 4 (PDCD4), suggesting the tumor-initiation ability of ABAQ.

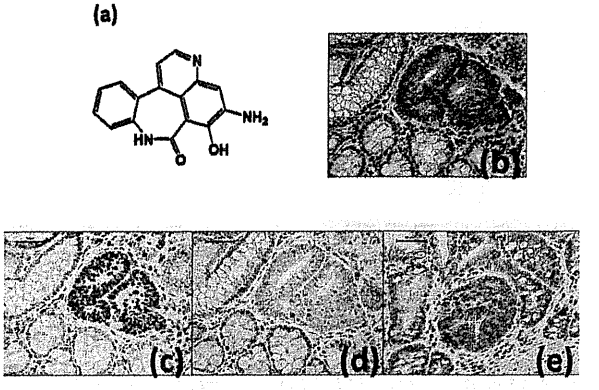

Fig. 1. (a) Chemical structure of ABAQ (ABAQ, $C_{16}H_{11}N_3O_2$, MW = 277.28). (b) A high-grade colonic dysplasia on H&E-stained section from a mouse in group 2 (200 ppm ABAQ + DSS). *Note*: Nuclear atypia in the crypts and Paneth's granules (red in color) in the cytoplasm of some dysplastic crypt cells. H&E stain; bar, 50 μm. (c) Many nuclei in the high-grade dysplasia in a serial section from (b) are positive for MCM2. MCM2 immunohistochemistry; bar, 50 μm. (d) Most nuclei in the high-grade dysplasia in a serial section from (b) are negative for PDCD4, whereas the nuclei in the surrounding normal crypts are positive for PDCD4. PDCD4 immunohistochemistry; bar, 50 μm. (e) The cytoplasmic expression of β-catenin is present in the high-grade dysplasia lesion developed in the colon of a mouse from group 2 (200 ppm ABAQ + DSS). Some nuclei are weakly positive for β-catenin. β-Catenin immunohistochemistry; bar, 50 μm. (For interpretation of the references to color in this figure legend, the reader is referred to the web version of the article.)

2. Materials and methods

2.1. Animals, chemicals and diet

Male Crlj: CD-1 (ICR) mice (Charles River Japan, Tokyo, Japan) 5 weeks of age were used. The mice were maintained at Gifu University Animal Facility according to the Institutional Animal Care Guidelines. All animals were housed in plastic cages (3 or 4 mice/cage) with free access to drinking water and a pelleted basal diet, CRF-1 (Oriental Yeast, Tokyo, Japan), under controlled conditions of humidity (50 ± 10%), light (12/12-h light/dark cycle) and temperature (23 ± 2 °C). After seven days of quarantine, they were randomized according to body weight into experimental and control groups. ABAQ was synthesized as previously described [7]; its purity was confirmed to be > 99% by HPLC. DSS with a molecular weight of 36,000–50,000 (Cat No. 160110) was purchased from MP Biochemicals, LLC (Aurora, OH, USA).

Table 1
Body, liver and relative liver weights and colon lengths in all groups.

Group no.	Treatment (no. of mice examined)	Body weight (g)	Liver weights (g)	Relative liver weight (g/100 g body weight)	Colon length (cm)
1	ABAQ [a] (100 mg/kg bw) → 2% DSS (15)	49.9 ± 7.29 [b]	2.5 ± 0.53 [c]	5.0 ± 0.48 [d]	16.5 ± 1.30 [c]
2	ABAQ (200 mg/kg bw) → 2% DSS (15)	44.8 ± 9.46	2.2 ± 0.56	4.8 ± 0.37 [c]	15.6 ± 1.31
3	ABAQ (200 mg/kg bw) (5)	42.0 ± 3.46	1.7 ± 0.23 [e]	4.1 ± 0.29	14.3 ± 0.42 [e]
4	Solvent → 2% DSS (5)	47.6 ± 1.62	2.1 ± 0.13	4.5 ± 0.35	15.9 ± 1.33
5	None (8)	51.6 ± 7.95	2.5 ± 0.45	4.8 ± 0.58	16.4 ± 1.21

[a] ABAQ, 5-amino-6-hydroxy-8*H*-benzo[6,7]azepino[5,4,3-*de*]quinolin-7-one; DSS, dextran sodium sulfate.
[b] Mean ± SD.
[c,d] Significantly different from group 3 ([c] $p < 0.05$ and [d] $p < 0.01$) according to a one-way ANOVA and the Tukey–Kramer Multiple Comparison test.
[e] Significantly different from group 5 ($p < 0.05$).

2.2. Experimental procedure for evaluating the tumor-initiating activity

The present study was approved by the Experimental Animal Research Committee of Gifu University. A total of 38 male ICR mice were divided into five experimental and solvent control groups. Groups 1 through 3 were treated with the single intragastric (i.g.) intubation of ABAQ at a dose of 100 or 200 mg/kg body weight. Starting one week after the ABAQ treatment, the animals in groups 1 ($n=15$) and 2 ($n=15$) were given 2% (w/v) DSS in drinking water for seven days, followed by no further treatments for 14 weeks. Groups 3 ($n=5$) and 4 ($n=5$) were given ABAQ (200 mg/kg body weight) alone and 2% DSS alone, respectively. Group 5 ($n=8$) was given solvent (physiological saline) alone and served as an untreated control group. All animals were sacrificed *via* CO_2 asphyxiation at week 16. The colons were flushed with saline, excised, measured for length (from the ileocecal junction to the anal verge), cut open longitudinally along the main axis and washed with saline. After carefully macroscopically inspecting the colons, the tissues were cut and fixed in 10% buffered formalin for at least 24 h. A histological examination was performed on paraffin-embedded sections following hematoxylin and eosin (H&E) staining. The presence or absence of mucosal ulceration, dysplasia and colonic neoplasms was examined according to our previous report [9]. A histopathological examination was also performed for other organs.

2.3. Immunohistochemistry of minichromosome maintenance protein 2 (MCM2), β-catenin and programmed cell death 4 (PDCD4)

We used paraffin-embedded sections of the colons of the mice in all groups for the immunohistochemical analysis. Serial histological sections (4 μm thickness) were made from each paraffin wax block. Immunohistochemical staining was performed automatically (Ventana Benchmark XTsystem; Ventana, Touchstone, Arizona, USA), according to the manufacturer's instructions. The primary antibodies were anti-MCM2 rabbit monoclonal antibody (no. 3619, anti-MCM2 (D7611)XP, 1:400 dilution; Cell Signaling Technology, Inc., Danvers, MA, USA), anti-β-catenin rabbit polyclonal antibody (#9661, 1:200 dilution; Cell Signaling Technology) and anti-PCDC4 rabbit polyclonal antibody (ab51495, 1:500 dilution; Abcam, Inc. Cambridge, MA, USA). In each case, the positive and negative controls were run concurrently. As the final step, the sections were lightly counterstained with Mayer's hematoxylin (Merck, Tokyo, Japan).

Immunoreactivity for antibodies against MCM2, PDCD4 and β-catenin was assessed in the lesions (high-grade dysplasia) that developed in groups 1 through 3 using a microscope (Olympus BX41, Olympus Optical Co., Tokyo, Japan). The intensity and localization of the immunoreactivity against the primary antibodies were determined by a pathologist (T.T.) who was unaware of the treatment group to which the slide belonged.

2.4. Statistical analysis

All measurements were compared using a one-way ANOVA with either Tukey's correction or Fisher's exact probability test (GraphPad Instat version 3.05, GraphPad Software, San Diego, CA), with a value of $p < 0.05$ as the criterion for significance.

3. Results

3.1. General observations

As listed in Table 1, the mean liver ($p < 0.05$) and relative liver weights ($p < 0.01$), and mean colon length ($p < 0.05$) in group 1 (100 mg/kg ABAQ + 2% DSS) were significantly larger than those observed in group 3 (200 mg/kg ABAQ alone). The mean liver weight and colon length of group 3 were significantly lower than that of group 5 (solvent control) ($p < 0.05$ for each comparison).

3.2. Pathological findings of the liver and colorectum of mice treated with ABAQ and/or DSS

There were no tumors in any organs, including the colorectum, in all groups. Fatty changes were observed in the liver of two mice (13%) in group 1, but not in other groups. As indicated in Table 2, colonic dysplasia (high-grade, Fig. 1b) developed in groups 1 through 3. DSS exposure increased the multiplicity of high-grade dysplasia induced by ABAQ. There were no dysplastic lesions in the mice in groups 4 and 5.

Table 2
Incidence and multiplicity of colonic lesions in the mice in each group.

Group no.	Treatment (no. of mice examined)	Mucosal ulcer	High-grade dysplasia
1	ABAQ [a] (100 mg/kg bw) → 2% DSS (15)	10/15 (67%) 1.40 ± 1.18 [b]	4/15 (27%) [c, d] 0.53 ± 1.13
2	ABAQ (200 mg/kg bw) → 2% DSS (15)	11/15 (73%) 1.27 ± 1.16	10/15 (67%) [e] 1.60 ± 1.50
3	ABAQ (200 mg/kg bw) (5)	0/5 (0%) 0	1/5 (20%) 0.20 ± 0.45
4	Solvent → 2% DSS (5)	5/5 (100%) 1.80 ± 0.84 [f]	0/5 (0%) 0
5	None (8)	0/8 (0%) 0	0/8 (0%) 0

[a] ABAQ, 5-amino-6-hydroxy-8*H*-benzo[6,7]azepino[5,4,3-*de*]quinolin-7-one; DSS, dextran sodium sulfate.
[b] Mean ± SD.
[c,d,e] Significantly different from group 2 ([c] $p < 0.05$), group 3 ([d] $p < 0.05$) and group 4 ([e] $p < 0.05$) according to the Fisher's exact probability test.
[f] Significantly different from group 5 ($p < 0.05$) according to a one-way ANOVA and the Tukey–Kramer Multiple Comparison test.

3.3. Immunohistochemical expression of MCM2, β-catenin, and PDCD4 in the high-grade dysplasia lesions

The nuclei in the high-grade dysplasia lesions were positive for MCM2 (Fig. 1c), reflecting a high proliferation activity, and negative for PDCD4 (Fig. 1d). A cytoplasmic and nuclear expression of β-catenin was observed in the high-grade dysplasia lesions (Fig. 1e).

4. Discussion

In this study, we confirmed the tumor-initiating ability of ABAQ in an inflammation-associated, two-stage mouse carcinogenesis model. Importantly, ABAQ treatment alone produced lesions exhibiting high-grade dysplasia lesions that are preneoplastic for colorectal cancer, although the incidence and multiplicity were low and statistically insignificant from group 5 (untreated control). One week of exposure to DSS after the single i.g. administration of ABAQ increased the incidence and number of high-grade dysplasia lesions in the colorectum. The dysplasia-inducing potency was considered to be dose-dependent, although only two doses of ABAQ were applied in this study.

In this study, dosing of ABAQ (100 mg/kg) followed by DSS (group 1) increased the liver weight, while 200 mg/kg of ABAQ (group 2) did not. However, both doses of ABAQ increased the relative liver weight. Fatty degeneration observed in the liver of a few mice of group 1 may be related to these changes. As to the colon length, the treatment of ABAQ alone (group 3) shortened the colon, suggesting pro-inflammatory action of ABAQ, but the colon lengths of groups 1 and 2 were increased when given DSS. In order to proof the dose dependency and discard the possible pro-inflammatory effect at higher doses of ABAQ, which might contribute to the tumor development, it would be interesting to use three or four different doses (from 50 to 200 mg/kg, for instance). Such an experiment is planned in our laboratory.

The Maillard reaction *in vivo* is involved in aging [12] and a variety of chronic diseases, such as diabetes and related retinopathy and nephropathy [13]. Pyrraline is formed as an advanced glycation end product in the Maillard reaction between glucose and the ε-amino group of lysine under physiological conditions [14]. The serum [15] and urine [16] concentrations of pyrraline are known to be increased in diabetic patients, and pyrraline is detected in individuals with diabetic glomerulosclerosis [17]. Epidemiological [18,19] and experimental investigations [20,21] have indicated a positive association between diabetes and cancer development in several tissues, including the colorectum, suggesting that certain chemicals formed by the Maillard reaction in the body increase the risk of cancer in patients with diabetes. However, little is known about mutagens formed through the Maillard reaction *in vivo*.

In this study, we observed high-grade dysplasia in the colorectum of the mice treated with ABAQ alone and ABAQ followed by DSS exposure. Although no colorectal neoplasms developed, these findings are of importance since high-grade dysplasia is known to be a precursor lesion of inflammatory conditions in the colon, such as inflammatory bowel disease (IBD) [22]. In the fact, the high-grade dysplasia observed in this study increased the degree of proliferation, as estimated on MCM2 immunohistochemistry, and altered the expression of β-catenin in the cytoplasm and nuclei. More importantly, almost null expression of PDCD4 was observed in the high-grade dysplasia lesions. This finding is in accordance with the results showing a negative expression of PDCD4 in patients with sporadic colorectal cancer [23,24], IBD-related colorectal cancer [22,25] and dysplasia in IBD [22,25].

In conclusion, the results of the current study indicate the potential tumor-initiating activity of ABAQ in the colon, with and without inflammation. Although the ABAQ level has not been determined in healthy subjects, ABAQ is a potential novel endogenous mutagen and tumor-initiating compound, as shown in this study and a previous investigation [7]. Since the mutagenic activity of ABAQ is comparable to that of PhIP [7], additional studies of the carcinogenicity of ABAQ in the colon and other tissues are required. Our findings provide a scientific basis for further research on the involvement of ABAQ in human health.

Conflict of interest

The authors declare no financial or commercial conflicts of interests.

Acknowledgments

This work was partly supported by a Grant-in-Aid for the 3rd Terms Comprehensive 10-Year Strategy for Cancer Control from the Ministry of Health, Labour and Welfare of Japan, Grants-in-Aid from Scientific Research from the Ministry of Education, Culture, Sports, Science, and Technology of Japan, Grants-in-Aid for National Cancer Center Research and Development Fund, Grants-in-Aid for the

U.S.-Japan Cooperative Medical Science Program, from the Ministry of Health, Labor and Welfare of Japan, and a grant from Takeda Science Foundation.

References

[1] T. Tanaka, M. Shimizu, T. Kohchi, H. Moriawaki, Chemical-induced carcinogenesis, J. Exp. Clin. Med. 5 (2013) 203–209.
[2] T. Sugimura, K. Wakabayashi, H. Nakagama, M. Nagao, Heterocyclic amines: mutagens/carcinogens produced during cooking of meat and fish, Cancer Sci. 95 (2004) 290–299.
[3] K. Wakabayashi, M. Nagao, H. Esumi, T. Sugimura, Food-derived mutagens and carcinogens, Cancer Res. 52 (1992) 2092s–2098s.
[4] IARC, Some Naturally Occurring Substances: Food Items and Constituents, Heterocyclic Aromatic Amines and Mycotoxins, IARC, WHO, Lyon, 1993, pp. 599.
[5] NTP, NTP 12th Report on Carcinogens, Rep Carcinog 12 (2011), iii-499.
[6] M. Jagerstad, K. Olsson, S. Grivas, C. Negishi, K. Wakabayashi, M. Tsuda, S. Sato, T. Sugimura, Formation of 2-amino-3,8-dimethylimidazo[4,5-f]quinoxaline in a model system by heating creatinine, glycine and glucose, Mutat. Res. 126 (1984) 239–244.
[7] R. Nishigaki, T. Watanabe, T. Kajimoto, A. Tada, T. Takamura-Enya, S. Enomoto, H. Nukaya, Y. Terao, A. Muroyama, M. Ozeki, M. Node, T. Hasei, Y. Totsuka, K. Wakabayashi, Isolation and identification of a novel aromatic amine mutagen produced by the Maillard reaction, Chem. Res. Toxicol. 22 (2009) 1588–1593.
[8] Y. Totsuka, T. Watanabe, S. Coulibaly, S. Kobayashi, M. Nishizaki, M. Okazaki, T. Hasei, K. Wakabayashi, H. Nakagama, In vivo genotoxicity of a novel heterocyclic amine, aminobenzoazepinoquinolinone-derivative (ABAQ), produced by the Maillard reaction between glucose and l-tryptophan, Mutat. Res. 760 (2014) 48–55.
[9] T. Tanaka, H. Kohno, R. Suzuki, Y. Yamada, S. Sugie, H. Mori, A novel inflammation-related mouse colon carcinogenesis model induced by azoxymethane and dextran sodium sulfate, Cancer Sci. 94 (2003) 965–973.
[10] T. Tanaka, R. Suzuki, H. Kohno, S. Sugie, M. Takahashi, K. Wakabayashi, Colonic adenocarcinomas rapidly induced by the combined treatment with 2-amino-1-methyl-6-phenylimidazo[4,5-b]pyridine and dextran sodium sulfate in male ICR mice possess beta-catenin gene mutations and increases immunoreactivity for beta-catenin, cyclooxygenase-2 and inducible nitric oxide synthase, Carcinogenesis 26 (2005) 229–238.
[11] H. Kohno, Y. Totsuka, Y. Yasui, R. Suzuki, S. Sugie, K. Wakabayashi, T. Tanaka, Tumor-initiating potency of a novel heterocyclic amine, aminophenylnorharman in mouse colonic carcinogenesis model, Int. J. Cancer 121 (2007) 1659–1664.
[12] D. Aronson, Pharmacological prevention of cardiovascular aging—targeting the Maillard reaction, Br. J. Pharmacol. 142 (2004) 1055–1058.
[13] D.R. McCance, D.G. Dyer, J.A. Dunn, K.E. Bailie, S.R. Thorpe, J.W. Baynes, T.J. Lyons, Maillard reaction products and their relation to complications in insulin-dependent diabetes mellitus, J. Clin. Invest. 91 (1993) 2470–2478.
[14] P.R. Smith, H.H. Somani, P.J. Thornalley, J. Benn, P.H. Sonksen, Evidence against the formation of 2-amino-6-(2-formyl-5-hydroxymethyl-pyrrol-1-yl)-hexanoic acid ('pyrraline') as an early-stage product or advanced glycation end product in non-enzymic protein glycation, Clin. Sci. (Lond.) 84 (1993) 87–93.
[15] H. Odani, T. Shinzato, Y. Matsumoto, I. Takai, S. Nakai, M. Miwa, N. Iwayama, I. Amano, K. Maeda, First evidence for accumulation of protein-bound and protein-free pyrraline in human uremic plasma by mass spectrometry, Biochem. Biophys. Res. Commun. 224 (1996) 237–241.
[16] M. Portero-Otin, R. Pamplona, M.J. Bellmunt, M. Bergua, R.H. Nagaraj, J. Prat, Urinary pyrraline as a biochemical marker of non-oxidative Maillard reactions in vivo, Life Sci. 60 (1997) 279–287.
[17] S. Miyata, V. Monnier, Immunohistochemical detection of advanced glycosylation end products in diabetic tissues using monoclonal antibody to pyrraline, J. Clin. Invest. 89 (1992) 1102–1112.
[18] M. Inoue, M. Iwasaki, T. Otani, S. Sasazuki, M. Noda, S. Tsugane, Diabetes mellitus and the risk of cancer: results from a large-scale population-based cohort study in Japan, Arch. Intern. Med. 166 (2006) 1871–1877.
[19] H. Yuhara, C. Steinmaus, S.E. Cohen, D.A. Corley, Y. Tei, P.A. Buffler, Is diabetes mellitus an independent risk factor for colon cancer and rectal cancer? Am. J. Gastroenterol. 106 (2011) 1911–1921, quiz 1922.
[20] K. Hata, M. Kubota, M. Shimizu, H. Moriwaki, T. Kuno, T. Tanaka, A. Hara, Y. Hirose, Monosodium glutamate-induced diabetic mice are susceptible to azoxymethane-induced colon tumorigenesis, Carcinogenesis 33 (2012) 702–707.
[21] M. Shimizu, Y. Shirakami, J. Iwasa, M. Shiraki, Y. Yasuda, K. Hata, Y. Hirose, H. Tsurumi, T. Tanaka, H. Moriwaki, Supplementation with branched-chain amino acids inhibits azoxymethane-induced colonic preneoplastic lesions in male C57BL/KsJ-db/db mice, Clin. Cancer Res. 15 (2009) 3068–3075.
[22] T. Tanaka, S. Sugie, Recent advances in pathobiology and histopathological diagnosis of inflammatory bowel disease, Pathol. Discov. 1 (2013) 1–6.
[23] M. Fassan, M. Pizzi, L. Giacomelli, C. Mescoli, K. Ludwig, S. Pucciarelli, M. Rugge, PDCD4 nuclear loss inversely correlates with miR-21 levels in colon carcinogenesis, Virchows Arch. 458 (2011) 413–419.
[24] G. Mudduluru, F. Medved, R. Grobholz, C. Jost, A. Gruber, J.H. Leupold, S. Post, A. Jansen, N.H. Colburn, H. Allgayer, Loss of programmed cell death 4 expression marks adenoma-carcinoma transition, correlates inversely with phosphorylated protein kinase B, and is an independent prognostic factor in resected colorectal cancer, Cancer 110 (2007) 1697–1707.
[25] K. Ludwig, M. Fassan, C. Mescoli, M. Pizzi, M. Balistreri, L. Albertoni, S. Pucciarelli, M. Scarpa, G.C. Sturniolo, I. Angriman, M. Rugge, PDCD4/miR-21 dysregulation in inflammatory bowel disease-associated carcinogenesis, Virchows Arch. 462 (2013) 57–63.

Mutation Research 760 (2014) 48–55

Contents lists available at ScienceDirect

Mutation Research/Genetic Toxicology and Environmental Mutagenesis

journal homepage: www.elsevier.com/locate/gentox
Community address: www.elsevier.com/locate/mutres

In vivo genotoxicity of a novel heterocyclic amine, aminobenzoazepinoquinolinone-derivative (ABAQ), produced by the Maillard reaction between glucose and L-tryptophan

Yukari Totsuka[a,*], Tetsushi Watanabe[b], Souleymane Coulibaly[b], Sae Kobayashi[b], Marina Nishizaki[b], Miho Okazaki[b], Tomohiro Hasei[b], Keiji Wakabayashi[c], Hitoshi Nakagama[a]

[a] *Division of Cancer Development System, National Cancer Center Research Institute, Chuo-ku, Tokyo, Japan*
[b] *Kyoto Pharmaceutical University, 1 Shichono-cho, Misasagi, Yamashina-ku, Kyoto 607-8412, Japan*
[c] *Graduate Division of Nutritional and Environmental Sciences, University of Shizuoka, Yada, Shizuoka, Japan*

ARTICLE INFO

Article history:
Received 1 October 2013
Received in revised form 2 December 2013
Accepted 4 December 2013
Available online 12 December 2013

Keywords:
Maillard reaction product
Micronucleated erythrocytes
Comet assay
gpt delta transgenic mice
Diabetes mellitus (DM)

ABSTRACT

We recently demonstrated that a novel heterocyclic amine, 5-amino-6-hydroxy-8*H*-benzo[6,7]azepino[5,4,3-*de*]quinolin-7-one (ABAQ), is produced from glucose and L-tryptophan by the Maillard reaction at physiological temperature and pH, and that ABAQ was strongly mutagenic for *Salmonella* strains in the presence of S9 mix. Here, we present the results of three *in vivo* genotoxicity assays of ABAQ. The comet assay revealed that DNA damage was significantly increased in the livers, kidneys, lungs, and bone marrows of ICR mice, 3 h after i.p. injection of ABAQ (50 mg/kg body weight (bw)). To evaluate clastogenicity, the peripheral blood micronucleus test was performed, also in ICR mice. ABAQ induced micronucleated reticulocytes (MNRETs) in a dose-dependent manner; the frequency of MNRETs was significantly elevated at all i.p. doses (12.5, 25, and 50 mg/kg bw) after 48 h. To investigate the mutagenicity of ABAQ *in vivo*, *gpt* delta transgenic mice were treated with five consecutive administrations of ABAQ by gavage at doses of 25 or 50 mg/kg per week for 3 weeks. The frequencies of *gpt* mutations (MF) in the liver of mice increased significantly compared with controls, in a dose-dependent manner. No significant increase of *gpt* MF was detected in the kidneys. Base substitutions predominated; both G:C→A:T and A:T→C:G mutations were significantly increased by ABAQ. The Spi⁻ MF was also significantly increased in the liver after ABAQ treatment. If formed *in vivo*, ABAQ may give rise to adverse genotoxic effects.

1. Introduction

Diabetes mellitus (DM) affects more than 300 million people worldwide and the number is predicted to increase to at least 400 million by 2030 [1]. Epidemiological studies show that diabetes patients have an increased incidence of cancers in certain organs, including liver, pancreas, kidney, and endometrium [2–5]; however, the causal mechanisms are not fully elucidated. A consistent increase in blood sugar levels is characteristic of diabetes, and the Maillard reaction is considered to be implicated in diabetic complications [6]. The Maillard reaction comprises a series of complex non-enzymatic reactions between the carbonyl group of a reducing sugar and the amino groups of amino acids, peptides, or proteins to yield an unstable Schiff base, which then leads to a relatively stable ketoamine known as an Amadori product [7]. The Amadori products react with amino acids or are converted into reactive carbonyl species, such as deoxyglucosone. During the latter stage of the reaction, the carbonyl species react with amino groups in proteins and other molecules.

We recently found that the Maillard reaction of glucose and L-tryptophan at physiological temperature and pH (37 °C and pH 7.4) produces mutagens, and we identified a novel heterocyclic amine,

Abbreviations: ABAQ, 5-amino-6-hydroxy-8*H*-benzo[6,7]azepino[5,4,3-*de*]quinolin-7-one; MNRETs, micronucleated reticulocytes; MF, mutation frequencies; DM, diabetes mellitus; PhIP, 2-amino-1-methyl-6-phenylimidazo[4,5-*b*]pyridine; *gpt*, guanine phosphoribosyltransferase; LMP, low melting point; NMP, normal melting point; DMSO, dimethyl sulfoxide; 6-TG, 6-thioguanine; SD, standard deviation; HCAs, heterocyclic amines.

* Corresponding author at: Division of Cancer Development System, National Cancer Center Research Institute, 1-1, Tsukiji 5-chome, Chuo-ku, Tokyo 104-0045, Japan. Tel.: +81 3 3547 52014552; fax: +81 3 3542 2530.
E-mail address: ytotsuka@ncc.go.jp (Y. Totsuka).

1383-5718/$ – see front matter © 2013 Elsevier B.V. All rights reserved.
http://dx.doi.org/10.1016/j.mrgentox.2013.12.002

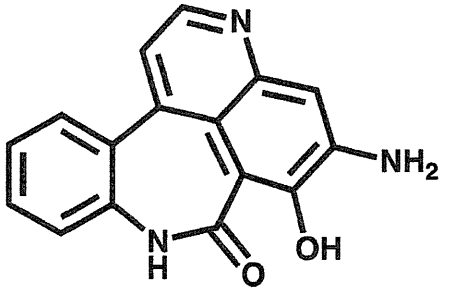

Fig. 1. Chemical structure of 5-amino-6-hydroxy-8*H*-benzo[6,7]azepino[5,4,3-*de*]quinolin-7-one (ABAQ).

5-amino-6-hydroxy-8*H*-benzo[6,7]azepino[5,4,3-*de*]quinolin-7-one (ABAQ, Fig. 1), from the reaction mixture [8]. A plausible mechanism for the formation of ABAQ from glucose and L-tryptophan is also shown in our previous report [8]. ABAQ induced mutations in *Salmonella typhimurium* strains TA98, TA100, YG1024, and YG1029 in the presence of S9 mix, and the mutagenic potency was the highest in YG1024, a derivative of TA98 that overproduces *O*-acetyltransferase. These results suggest that ABAQ mutagenicity depends on metabolic activation catalyzed by cytochrome P450 and *O*-acetyltransferase [8]. These characteristics are very similar to those of a cooked food-derived heterocyclic amine, 2-amino-1-methyl-6-phenylimidazo[4,5-*b*]pyridine (PhIP), suggested to be formed by the reaction of creatine with Maillard reaction products from glucose and phenylalanine by heating at high temperatures [9]. The mutagenic potencies of ABAQ in TA98 and YG1024 are comparable to those of PhIP [8].

Because ABAQ was discovered only recently, its biological activities have not been determined, aside from *Salmonella* mutagenicity. In the present study, therefore, we have examined the genotoxicity of ABAQ *in vivo*, and compared it to that of PhIP; the acute studies used the micronucleus and comet assays; chronic mutagenicity was evaluated using the *gpt* delta transgenic mouse system, in which point mutations and deletions can be assessed by *gpt* and Spi$^-$ selection, respectively [10,11]. We show here that ABAQ induces acute and chronic genotoxicity, and discuss the possible underlying mechanisms.

2. Materials and methods

2.1. Chemicals

ABAQ (more than 99% pure) was obtained from Hamari Chemicals, Ltd. (Osaka, Japan). Corn oil, low melting point (LMP) and normal melting point (NMP) agarose, dimethyl sulfoxide (DMSO), and Triton X-100 were purchased from Sigma–Aldrich (St. Louis, MO, USA). PhIP·HCl and other chemicals were purchased from Wako Pure Chemical Industries (Osaka, Japan).

2.2. Experimental animals

Male ICR mice (6 weeks old) and guanine phosphoribosyltransferase (*gpt*) delta mice (6 weeks old) were purchased from Japan SLC (Shizuoka, Japan). The *gpt* delta mice carry approximately 80 copies of *lambda* EG10 DNA on chromosome 17 on a C57BL/6J background [12]. The animals were provided with food (CE-2 pellet diet; CLEA Japan, Inc., Tokyo, Japan) and tap water *ad libitum*, and maintained under controlled conditions as follows: a 12-h light/dark cycle, 22 ± 2 °C room temperature, and 55 ± 10% relative humidity. After quarantine for one week, the experiments were conducted according to the "Guidelines for Animal Experiments in the National Cancer Center or Kyoto Pharmaceutical University", and the animal studies were approved by its Experimental Animal Research Committee.

2.3. In vivo comet assay

The alkaline comet assay was performed according to a published method [13]. ABAQ was suspended in olive oil and 25, 50, or 100 mg/kg body weight (bw) doses were injected intraperitoneally (i.p.). PhIP was dissolved in physiological saline and administered i.p. to mice at 12.5, 25, or 50 mg/kg bw. Controls received olive oil or physiological saline i.p. Five ICR mice were used for each group. Liver, kidneys, lungs, and bone marrow were removed 3 h after the injections. Each organ, except for bone marrow, was minced, suspended in chilled homogenizing buffer (pH 7.5, 0.075 M KCl and 0.03 M sodium EDTA), and homogenized gently with a Dounce-type homogenizer. Normal melting point agarose (100 μl) was layered as the first layer on a glass slide; LMP agarose (50 μl) containing 1000 nuclei was layered next; normal melting point agarose (100 μl) was layered last. The slides were immersed in ice-cold lysing solution (pH 10, containing 2.5 M NaCl, 100 mM sodium EDTA, 10 mM Tris–HCl, 1% sodium N-lauryl sarcosinate, 10% DMSO and 1% Triton X-100) for 60 min. The slides were placed on a horizontal gel electrophoresis platform and covered with chilled alkaline solution (containing 300 mM NaOH, 1 mM sodium EDTA) for 20 min to allow for the DNA to unwind and expose alkali-labile sites. The nuclei were electrophoresed at 25 V (1 V/cm) for 20 min. After electrophoresis, the specimens were rinsed twice with 400 mM Tris–HCl (pH 7.5) to neutralize excess alkali, stained with 50 μl ethidium bromide solution, and covered with a cover slip. Nuclei (100 per organ per animal) were inspected using a fluorescence microscope equipped with a CCD camera. The tail moment of the DNA was measured using Komet Assay software (Kinetic Imaging Ltd., Liverpool, UK).

2.4. In vivo micronucleus test

The micronucleus test was carried out according to a published method [14]. ABAQ suspended in olive oil or PhIP dissolved in physiological saline were administered i.p. at 12.5, 25, or 50 mg/kg bw. Control mice were treated with either olive oil or physiological saline. Five ICR mice were used for each group. Peripheral blood (5 μl) was obtained from the ventral tail, spread on an acridine orange-coated glass slide, and covered with a cover slip. Supravitally stained reticulocytes were observed using a fluorescence microscope with a blue excitation and a yellow-to-orange barrier filter. The number of MNRETs per 1000 reticulocytes was scored for each mouse.

2.5. gpt and Spi$^-$ mutation assays

For mutation analysis, each group of five male *gpt* delta mice was orally administered five consecutive doses (25 or 50 mg/kg) of ABAQ per week for 3 weeks. The control mice ($n = 4$) were treated with solvent (corn oil) alone. The mice were sacrificed at 14 weeks age (5 weeks after ABAQ administration). Liver and kidneys were removed and stored at −80 °C until high-molecular-weight genomic DNA was extracted using a RecoverEase DNA Isolation Kit (Agilent Technology, USA) according to the manufacturer's instructions. *Lambda* EG10 phages were rescued using Transpack Packaging Extract (Stratagene, La Jolla, CA). The *gpt* and Spi$^-$ mutagenesis assays were performed according to published methods [12]. Briefly, *E. coli* YG6020 was infected with the phage and spread on M9 salt plates containing chloramphenicol (Cm) and 6-thioguanine (6-TG) and incubated for 72 h at 37 °C to select for colonies harboring a plasmid carrying the gene encoding chloramphenicol acetyltransferase, as well as a mutated *gpt*. The

6-TG-resistant isolates were cultured overnight at 37 °C in LB broth containing 25 mg/mL Cm, harvested by centrifugation (7000 rpm, 10 min), and stored at −80 °C.

The mutational spectra of 6-TG coding sequences were determined using PCR and direct sequencing, and a 739-bp DNA fragment containing *gpt* was amplified by PCR as described previously [12]. Sequence analysis was performed at Takara Bio Inc. (Mie, Japan). The Spi⁻ assay was performed as described previously [11,12]. The lysates of Spi⁻ mutants were obtained by infection of *E. coli* LE392 with the recovered Spi⁻ mutants.

2.6. Statistical analysis

Comet assay and micronucleus test data are expressed as means ± standard deviation (SD). Student's *t*-test was used to evaluate the significance of differences of DNA tail moment in the comet assay and the frequency of MNRETs in the micronucleus test between groups treated with ABAQ, PhIP, and control groups. The data from the *gpt* and Spi⁻ mutation assays were expressed as means ± SD. The data were compared with the corresponding solvent control using the F test before application of the Student's *t*-test. Mutational spectra were compared using Fisher's exact test [15]. *P* values lower than 0.05 were considered to indicate statistical significance.

3. Results

3.1. Analysis of acute DNA-damaging activity of ABAQ and PhIP in multiple organs (in vivo comet assay)

DNA damage induced by ABAQ and PhIP in multiple organs (liver, kidneys, lungs, and bone marrow) was evaluated as the DNA tail moment, 3 h after i.p. administration, using the comet assay under alkaline conditions. As shown in Fig. 2, the DNA tail moment values increased in a dose-dependent manner following ABAQ treatment, and the values for all organs were significantly higher at 50 and 100 mg/kg bw compared with those of control mice. High mean tail moments were detected in the bone marrow of mice treated with 50 and 100 mg/kg bw and DNA damage values were 1.3- and 1.4-fold higher, respectively compared with the control ($P < 0.01$ at both doses). For PhIP, a significant increase of DNA tail moment values was detected in all organs examined at 12.5, 25, and 50 mg/kg bw. The highest tail moment was detected in the kidneys at 50 mg/kg bw and the DNA damage was 1.3-fold ($P < 0.01$) higher than that of the control group.

3.2. Clastogenicity of ABAQ and PhIP in peripheral blood (in vivo micronucleus test)

The clastogenic activities of ABAQ and PhIP were examined by the micronucleus test. Frequencies of MNRETs were increased dose-dependently, 24 h and 48 h after the administration of ABAQ, and the frequencies were significantly elevated at all doses examined (12.5, 25, and 50 mg/kg bw) at 48 h. The highest frequencies of MNRETs were detected at 48 h, and the frequencies were 3.0-, 4.2-, and 5.8-fold higher than controls at 12.5, 25, and 50 mg/kg bw, respectively ($P < 0.01$ at each dose). Similarly, the frequency of MNRETs was dose-dependently increased 24 and 48 h after injection of PhIP, and was the highest at 50 mg/kg bw at 48 h after administration; the value was 7.4-times higher than that of controls ($P < 0.01$) (Fig. 3).

3.3. gpt and Spi⁻ mutations in the liver and kidneys of gpt transgenic mice treated with ABAQ

3.3.1. General observations of gpt delta transgenic mice administrated ABAQ

Body weights of *gpt* delta mice receiving vehicle control reached 27.5 ± 3.1 g, 30 d after gastric intubation. Values for *gpt* delta mice receiving multiple doses of ABAQ at 25 or 50 mg/kg bw were 28.7 ± 2.3 g and 28.5 ± 1.5 g, respectively, 30 d after administration, and no significant difference was observed compared with the vehicle control group. The average dietary consumption per day per mouse was about 3 g and was not affected by ABAQ.

3.3.2. gpt mutations in the liver and kidneys of gpt transgenic mice following ABAQ treatment

To determine the mutagenic effects of ABAQ in the liver and kidneys, *gpt* delta transgenic mice were treated with low or high doses of ABAQ (five consecutive administrations of ABAQ by gavage of 25 or 50 mg/kg bw per week for 3 weeks). Data are summarized in Table 1 and Fig. 4. MFs in the liver induced by both doses of ABAQ were significantly increased, 3.3- or 3.6-fold compared with the vehicle controls (Fig. 4A). In contrast, there was no increase in the MF in the kidneys following the low dose of ABAQ. The high dose of ABAQ resulted in a slight increase in the MF, but it was not statistically significant (Fig. 4B).

PCR and DNA sequence analyses revealed 42 and 14 independent 6-TG-resistant mutations induced by ABAQ and in the vehicle controls, respectively. The classes of *gpt* mutations are summarized in Table 2. Because our control samples were limited, previously

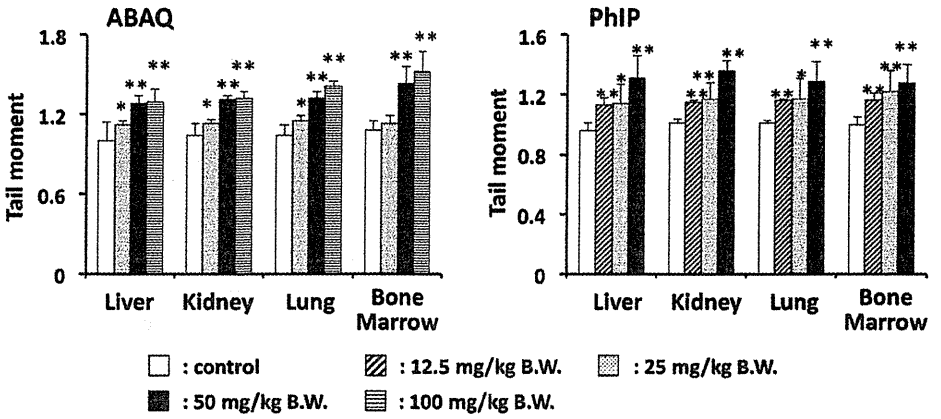

Fig. 2. DNA-damaging activity of ABAQ and PhIP in various organs of mice. Mice were injected i.p. with four doses of either ABAQ or PhIP. Control mice were treated with olive oil or physiological saline. Organs were removed at 3 h after the injection. The values represent the mean of five mice ± SD. Tail moment values of organs untreated mice for ABAQ and PhIP experiments were as follows: liver (1.00 ± 0.14 and 0.96 ± 0.05), kidney (1.04 ± 0.09 and 1.01 ± 0.03), lung (1.04 ± 0.08 and 1.01 ± 0.02), bone marrow (1.08 ± 0.07 and 1.00 ± 0.05). *$P < 0.05$ (*vs.* control), **$P < 0.01$ (*vs.* control).

Table 1
Summary of *gpt* mutation frequency in the liver and kidneys of *gpt* delta mice treated with ABAQ.

	Mouse ID	Number of colonies		MF ($\times 10^{-6}$)	Average MF ($\times 10^{-6}$)[a]
		Mutant	Total		
Liver					
[b]Control	1	5	907,500	5.51	
	2	5	892,500	5.60	
	3	1	862,500	1.16	
	4	3	627,000	4.78	
	Total	14	3,289,500		4.26 ± 2.10
ABAQ					
25 mg/kg × 5	1	8	361,500	22.13	
	2	1	613,500	1.63	
	3	6	625,500	9.59	
	4	10	453,000	22.08	
	5	7	463,500	15.10	
	Total	32	2,517,000		14.11 ± 8.73*
50 mg/kg × 5	1	14	1,129,500	12.39	
	2	10	978,000	10.22	
	3	14	1,003,500	13.95	
	4	27	1,137,000	23.75	
	5	15	922,500	16.26	
	Total	80	5,170,500		15.32 ± 5.20**
Kidneys					
[b]Control	1	4	709,500	5.64	
	2	4	366,000	10.93	
	3	3	384,000	17.81	
	4	5	361,500	13.83	
	Total	16	1,821,000		9.55 ± 3.58
ABAQ					
25 mg/kg × 5	1	8	928,500	6.46	
	2	5	715,500	6.99	
	3	3	519,000	5.78	
	4	14	991,500	14.12	
	5	9	571,500	15.75	
	Total	37	3,726,000		9.82 ± 4.72
50 mg/kg × 5	1	6	702,000	12.39	
	2	5	985,500	10.22	
	3	7	529,500	13.95	
	4	11	492,000	23.75	
	5	12	657,000	16.26	
	Total	41	3,366,000		13.49 ± 7.01

[a] Mean ± SD.
[b] Solvent control (corn oil).
* $P < 0.05$.
** $P < 0.01$ (*vs.* solvent control) by Student's *t*-test.

Table 2
Classification of *gpt* mutations detected in the liver of control and ABAQ-treated mice.

Type of mutation	Control		Control-2[a]		ABAQ		*P* value[b]
	No. of mutations (%)	Specific MF[c] ($\times 10^{-6}$)	No. of mutations (%)	Specific MF[c] ($\times 10^{-6}$)	No. of mutations (%)	Specific MF[c] ($\times 10^{-6}$)	
Base substitution							
Transition							
G:C to A:T	7(46.7)	2.13	21(42.9)	2.78	14(33.3)	5.77	0.02[d], 0.03[e]
A:T to G:C	0(0)	0.00	4(8.2)	0.53	3(7.1)	1.24	0.04[d], 0.25[e]
Transversion							
G:C to T:A	5(33.3)	1.52	5(10.2)	0.66	9(21.4)	3.71	0.10[d], 0.0005[e]
G:C to C:G	0(0)	0.00	2(4.1)	0.26	1(2.4)	0.41	0.24[d], 0.72[e]
A:T to T:A	0(0)	0.00	4(8.2)	0.53	4(9.5)	1.65	0.02[d], 0.09[e]
A:T to C:G	0(0)	0.00	1(2.0)	0.13	3(7.1)	1.25	0.04[d], 0.02[e]
Insertion	1(6.7)	0.30	1(2.0)	0.13	1(2.4)	0.41	0.83[d], 0.40[e]
Deletion	2(13.3)	0.61	6(12.2)	0.79	5(12.0)	2.06	0.12[d], 0.10[e]
Others	0(0)	0.00	5(10.2)	0.66	2(4.8)	0.82	0.10[d], 0.79[e]
Total	15[f](100)	4.56	49(100)	6.48	42(100)	17.30	0.00001[d], 0.00001[e]

[a] Data are from Masumura et al. [15].
[b] *P* values were determined using Fisher's exact test according to Carr and Gorelick [14].
[c] Specific MFs were calculated by multiplying the total mutation frequency by the ratio of each type of mutation to the total mutation.
[d] ABAQ *vs* control.
[e] ABAQ *vs* control-2.
[f] One animal had two mutations.

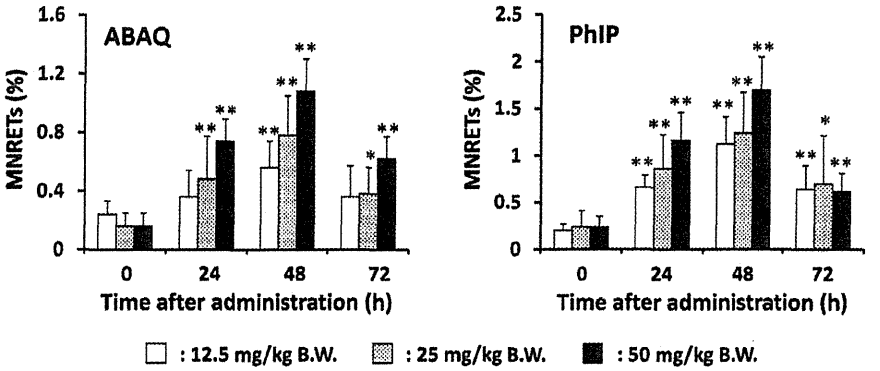

Fig. 3. Clastogenic activity of ABAQ and PhIP in peripheral blood of mice. Mice were injected i.p. with three doses of either ABAQ or PhIP. Control mice were treated with olive oil or physiological saline. One thousand reticulocytes were observed per mouse. The values represent the mean of five mice ± SD. *$P < 0.05$ (*vs.* control), **$P < 0.01$ (*vs.* control).

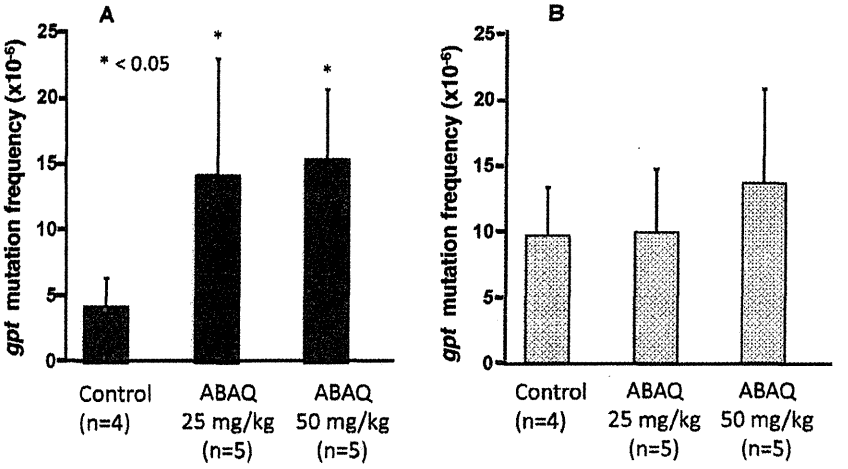

Fig. 4. The *gpt* MFs in the liver (A) and kidneys (B) of mice after multiple administration of ABAQ. Male mice were treated with multiple (25 or 50 mg/kg × 5 times per week for 3 weeks) doses of MGT, and mice were sacrificed 5 weeks after ABAQ administration. The data represent the mean ± SD. *$P < 0.05$, Student's *t*-test *versus* the corresponding vehicle-control mice.

published data [16] are also included in Table 2 (Control-2). Base substitutions predominated in both ABAQ-induced and spontaneous cases. G:C → A:T transitions and A:T → C:G transversions were significantly higher in the ABAQ-treated group.

3.3.3. *Spi⁻ mutations in the liver and kidneys of gpt transgenic mice following ABAQ treatment*

We also measured Spi⁻ MFs in the liver and kidneys of *gpt* delta mice treated with low and high doses of ABAQ (Table 3 and Fig. 5). The mean Spi⁻ MF values in the liver was $1.86 \pm 1.47 \times 10^{-6}$ (control), $6.17 \pm 2.49 \times 10^{-6}$ (low dose) and $6.81 \pm 2.57 \times 10^{-6}$ (high dose), respectively. Spi⁻ MFs in the liver of the both low- and high-dose groups were significantly elevated, up to 2-fold (Fig. 5A). Similar to liver MFs, in the kidneys, Spi⁻ MF showed around 3-fold increase, although this difference was not significant (Fig. 5B).

4. Discussion

The novel heterocyclic amine, ABAQ, identified as a product of the Maillard reaction at physiological temperature and pH, was genotoxic *in vivo*, as revealed by the comet assay, micronucleus test, and *gpt* and Spi⁻ mutation assays. The comet assay is a sensitive method for detecting DNA damages, including double- and single-strand DNA breaks, which are generated indirectly from incomplete excision repair and alkali-labile sites [17]. The DNA tail moment values for liver, kidneys, lungs, and bone marrow in ABAQ-treated (50 mg/kg bw) mice were significantly higher than those of mice treated similarly with PhIP, a representative mutagenic/carcinogenic heterocyclic amine. These results indicate that ABAQ and PhIP have similar levels of DNA-damaging activity in these organs. Under alkaline conditions, not only ABAQ-DNA adducts but also oxidative- and inflammation-related DNA adducts raised by the accompanying immunological response can be measured as DNA damage. ABAQ apparently induced DNA damage in various organs; however, the cause of the damage might be different in each organ. Further studies are required to elucidate this.

The micronucleus test is widely used to detect the clastogenicity of chemicals. Here we show that reticulocytes in the peripheral blood were supravitally stained with acridine orange, and MNRETs can be detected before being trapped and destroyed by the spleen [18]. The frequency of MNRETs was dose-dependently increased at 24 and 48 h after i.p. injection of ABAQ, and the highest frequency was found at 48 h after the injection. Similarly, frequencies of MNRETs increased dose-dependently 24 h and 48 h after PhIP treatment. For ABAQ, the highest frequency of MNRETs was detected 48 h after the injection of 50 mg/kg bw, similar to that observed at 48 h after the injection of 12.5 mg/kg bw PhIP. These results suggest that ABAQ is clastogenic in reticulocytes, with slightly lower potency than that of PhIP.

ABAQ-induced mutations in the liver included base substitutions and deletions. Despite the results of the comet assay, no significant increase of *gpt* and Spi⁻ MF was observed in the kidneys.

Table 3
Summary of Spi⁻ mutant frequency in the liver and kidneys of *gpt* delta mice treated with ABAQ.

	Mouse ID	Number of colonies		MF ($\times 10^{-6}$)	Average MF ($\times 10^{-6}$)[a]
		Mutant	Total		
Liver					
[b]Control	1	9	2,281,500	5.51	
	2	2	2,767,500	5.60	
	3	3	3,115,500	1.16	
	4	7	3,898,500	4.78	
	Total	21	12,063,000		1.86 ± 1.47
ABAQ					
25 mg/kg × 5	1	9	1,135,500	7.93	
	2	6	1,587,000	3.78	
	3	4	1,267,500	3.16	
	4	8	1,041,000	7.68	
	5	11	1,324,500	8.31	
	Total	38	6,355,500		6.17 ± 2.49**
50 mg/kg × 5	1	12	1,299,000	9.24	
	2	8	804,000	9.95	
	3	7	1,293,500	5.41	
	4	5	1,102,500	4.54	
	5	4	811,500	4.93	
	Total	36	5,310,500		6.81 ± 2.57**
Kidneys					
[b]Control	1	3	1,306,500	2.29	
	2	1	745,500	1.34	
	3	0	763,500	0.00	
	4	1	960,000	1.04	
	Total	5	3,775,500		1.17 ± 0.94
ABAQ					
25 mg/kg × 5	1	0	1,945,500	0.00	
	2	1	1,405,500	0.71	
	3	0	1,048,500	0.00	
	4	2	1,501,500	1.33	
	5	2	1,029,000	1.94	
	Total	5	6,930,000		0.80 ± 0.84
50 mg/kg × 5	1	4	867,000	4.61	
	2	1	1,017,000	0.98	
	3	2	700,500	2.86	
	4	5	790,500	6.33	
	5	1	933,000	1.07	
	Total	13	3,366,000		3.17 ± 1.72

[a] Mean ± SD.
[b] Solvent control (corn oil).
** $P < 0.01$ (*vs.* solvent control), Student's *t*-test.

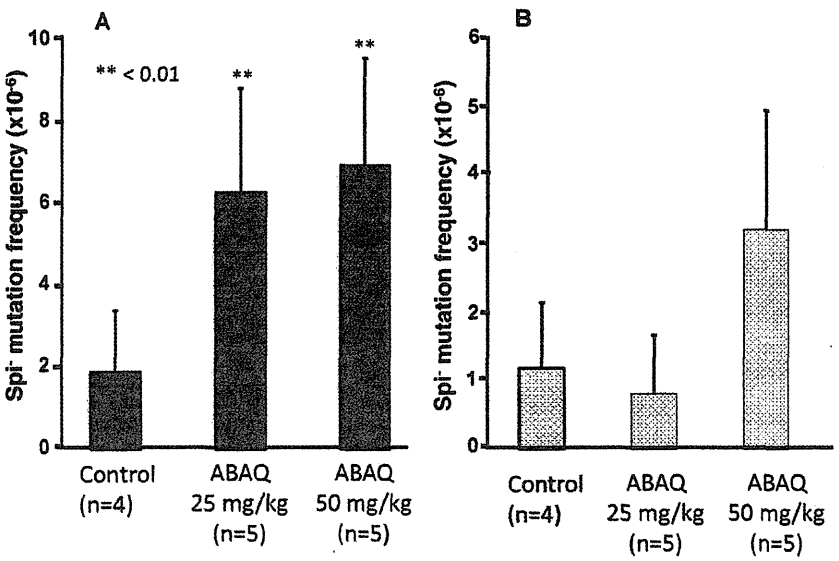

Fig. 5. The Spi⁻ MFs in the liver (A) and kidneys (B) of *gpt* delta mice exposed to multiple doses of ABAQ. An asterisk (*) denotes $P < 0.05$, Student's *t*-test for MFs of ABAQ-treated compared with the corresponding vehicle-control mice.

The reason is not fully understood yet; however, ABAQ administration routes might affect its *in vivo* genotoxicity. In the present study, i.p. injection was used for the comet and micronucleus assays, and i.g. intubation for the *gpt* and Spi$^-$ mutation assays. In general, the absorption rates following i.p. administration were more rapid than i.g. intubation. This may account for the higher genotoxicity of ABAQ observed in the micronucleus and comet assay compared with the results of the mutagenicity test in *gpt* delta mice. Both *gpt* and Spi$^-$ MFs in the kidneys observed in ABAQ-treated mice tended to increase, but this was not statistically significant (Figs. 4 and 5). We suggest, therefore, that ABAQ dosing using i.g. intubation may not be high enough for robust genotoxicity.

The *gpt* mutations induced in the liver are summarized in Table 2. Because our control samples were limited in number, we included and compared the data from a previous report (Control-2 [16]). In the mutation spectrum analysis, the most prominent mutation induced by ABAQ was G:C → A:T ($P < 0.05$) compared with both control groups. A previous study showed that ABAQ is mutagenic for *S. typhimurium* TA98 and YG1024 with S9 mix [8]. The sensitivity was much higher in YG1024 than in TA98, suggesting that *O*-acetyltransferase activity is required to activate ABAQ, as for other food-borne mutagenic compounds, such as heterocyclic amines (HCAs). The exocyclic amino group of HCAs binds guanine bases to form DNA adducts [19–22]. No data are available regarding the chemical structures of ABAQ-DNA adducts, except for the mutational spectral data for ABAQ. Therefore, we may conclude that the guanine base may be involved, to form ABAQ-DNA adducts. In addition, the G:C → A:T transition commonly occurs in spontaneous mutants, and deamination of 5-methylcytosine or alkylation of guanine might be involved in these mutations [23,24]. Moreover, inflammation may be involved [25]. In contrast, the frequencies of A:T → C:G transversions were also significantly different between ABAQ-treated and control groups. Even though its specific MF was low, this type of mutation is rare (almost none in the control cases). Therefore, it might be diagnostic for ABAQ-exposure. Further studies are required to determine the nature of the reactions that produce ABAQ-DNA adducts, and the resulting genotoxic mechanisms.

DM is a risk factor for various types of cancers [2–5], and researchers have focused on the relation between type-2 diabetes and cancer incidence. Evidence indicates that alterations in signal transduction pathways that promote cell proliferation caused by hyperglycemia, or insulin resistance and hyperinsulinemia associated with DM, promote oncogenesis [26–28]. However, whether diabetes initiates tumorigenesis is unknown. *In vivo* Maillard reactions are increased under diabetic conditions [29] and reaction products such as ABAQ may play a role in cancer etiology. A study on *in vivo* formation of ABAQ in diabetic model animals and diabetic patients is in progress in our laboratory. To understand the effect of ABAQ on DM-related cancer, it is important to evaluate the carcinogenicity of ABAQ using animal models. Moreover, epidemiological studies to evaluate the relation between ABAQ and DM-related cancer will also be required.

Conflict of interest statement

None.

Acknowledgments

We thank Naoaki Uchiya, Yoko Matsumoto, Kumi Otsuka and Aya Sakaizawa for excellent technical assistance. This study was supported by Grants-in-Aid for National Cancer Center Research and Development Fund, for the U.S. – Japan Cooperative Medical Science Program, from the Ministry of Health, Labor and Welfare of Japan and Scientific Research from the Ministry of Education, Culture, Sports, Science, and Technology of Japan.

References

[1] J.E. Shaw, R.A. Sicree, P.Z. Zimmet, Global estimates of the prevalence of diabetes for 2010 and 2030, Diabetes Res. Clin. Pract. 87 (2010) 4–14.
[2] C. Wang, X. Wang, G. Gong, Q. Ben, W. Qiu, Y. Chen, G. Li, L. Wang, Increased risk of hepatocellular carcinoma in patients with diabetes mellitus: a systematic review and meta-analysis of cohort studies, Int. J. Cancer 130 (2012) 639–1648.
[3] Q. Ben, M. Xu, X. Ning, Y. Wang, Y. Li, Diabetes mellitus and risk of pancreatic cancer: a meta-analysis of cohort studies, Eur. J. Cancer 47 (2011) 1928–1937.
[4] S.C. Larsson, A. Wolk, Diabetes mellitus and incidence of kidney cancer: a meta-analysis of cohort studies, Diabetologia 54 (2011) 1013–1018.
[5] M. Kasuga, K. Ueki, N. Tajima, M. Noda, K. Ohashi, H. Noto, A. Goto, W. Ogawa, R. Sakai, S. Tsugane, N. Hamajima, H. Nakagama, K. Tajima, K. Miyazono, K. Imai, Report of the Japan Diabetes Society/Japanese Cancer Association Joint Committee on Diabetes and Cancer, Cancer Sci. 104 (2013) 965–976.
[6] D.R. McCance, D.G. Dyer, J.A. Dunn, K.E. Bailie, S.R. Thorpe, J.W. Baynes, T.J. Lyons, Maillard reaction products and their relation to complications in insulin-dependent diabetes mellitus, J. Clin. Invest. 91 (1993) 2470–2478.
[7] J.E. Hodge, Dehydrated foods, chemistry of browning reactions in model systems, J. Agric. Food Chem. 1 (1953) 928–943.
[8] R. Nishigaki, T. Watanabe, T. Kajimoto, A. Tada, T. Takamura-Enya, S. Enomoto, H. Nukaya, Y. Terao, A. Muroyama, M. Ozeki, M. Node, T. Hasei, Y. Totsuka, K. Wakabayashi, Isolation and identification of a novel aromatic amine mutagen produced by the Maillard reaction, Chem. Res. Toxicol. 22 (2009) 1588–1593.
[9] M. Shioya, K. Wakabayashi, S. Sato, M. Nagao, T. Sugimura, Formation of a mutagen, 2-amino-1-methyl-6-phenylimidazo[4,5-*b*]pyridine (PhIP) in cooked beef, by heating a mixture containing creatinine, phenylalanine and glucose, Mutat. Res. 191 (1987) 133–138.
[10] T. Nohmi, K. Masumura, Molecular nature of intrachromosomal deletions and base substitutions induced by environmental mutagens, Environ. Mol. Mutagen. 45 (2005) 150–161.
[11] T. Nohmi, M. Suzuki, K. Masumura, M. Yamada, K. Matsui, O. Ueda, H. Suzuki, M. Katoh, H. Ikeda, T. Sofuni, Spi(−) selection: an efficient method to detect gamma-ray-induced deletions in transgenic mice, Environ. Mol. Mutagen. 34 (1999) 9–15.
[12] T. Nohmi, T. Suzuki, K. Masumura, Recent advances in the protocols of transgenic mouse mutation assays, Mutat. Res. 455 (2000) 191–215.
[13] M. Kawanishi, T. Watanabe, S. Hagio, S. Ogo, C. Shimohara, R. Jouchi, S. Takayama, T. Hasei, T. Hirayama, Y. Oda, T. Yagi, Genotoxicity of 3,6-dinitrobenzo[e]pyrene, a novel mutagen in ambient air and surface soil, in mammalian cell *in vitro* and *in vivo*, Mutagenesis 24 (2009) 279–284.
[14] M. Hayashi, T. Morita, Y. Kodama, T. Sofuni, M. Ishidate Jr., The micronucleus assay with mouse peripheral blood reticulocytes using acridine orange coated slides, Mutat. Res. 245 (1990) 245–249.
[15] G.J. Carr, N.J. Gorelick, Mutational spectra in transgenic animal research: data analysis and study design based upon the mutant or mutation frequency, Environ. Mol. Mutagen. 28 (1996) 405–413.
[16] K. Masumura, M. Horiguchi, A. Nishikawa, T. Umemura, K. Kanki, Y. Kanke, T. Nohmi, Low dose genotoxicity of 2-amino-3,8-dimethylimidazo[4,5-*f*]quinoxaline (MeIQx) in *gpt* delta transgenic mice, Mutat. Res. 541 (2003) 91–102.
[17] N.P. Singh, M.T. McCoy, R.R. Tice, E.L. Schneider, A simple technique for quantitation of low levels of DNA damage in individual cells, Exp. Cell Res. 175 (1988) 184–191.
[18] M. Hayashi, R.R. Tice, J.T. MacGregor, D. Anderson, D.H. Blakey, M. Kirsh-Volders, F.B. Oleson Jr., F. Pacchierotti, F. Romaga, H. Shimada, In vivo rodent erythrocyte micronucleus assay, Mutat. Res. 312 (1994) 293–304.
[19] T. Sugimura, K. Wakabayashi, H. Nakagama, M. Nagao, Heterocyclic amines: mutagens/carcinogens produced during cooking of meat and fish, Cancer Sci. 95 (2004) 290–299.
[20] R.J. Turesky, S.C. Rossi, D.H. Welti, J.O. Lay Jr., F.F. Kadlubar, Characterization of DNA adducts formed in vitro by reaction of N-hydroxy-2-amino-3-methylimidazo[4,5-*f*]quinoline and N-hydroxy-2-amino-3,8-dimethylimidazo[4,5-*f*]quinoxaline at the C-8 and N_2 atoms of guanine, Chem. Res. Toxicol. 5 (1992) 479–490.
[21] E.G. Snyderwine, P.P. Roller, R.H. Adamson, S. Sato, S.S. Thorgeirsson, Reaction of N-hydroxyamine and N-acetoxy derivatives of 2-amino-3-methylimidazo[4,5-*f*]quinoline with DNA. Synthesis and identification of N-(deoxyguanosin-8-yl)-IQ, Carcinogenesis 9 (1988) 1061–1065.
[22] H. Frandsen, S. Grivas, R. Anderson, L. Dragsted, J.C. Larsen, Reaction of the N 2-acetoxy derivative of 2-amino-1-methyl-6-phenylimidazo[4,5-*b*]pyridine (PhIP) with 2′-deoxyguanosine and DNA. Synthesis and identification of N 2-(2′-deoxyguanosine-8-yl)-PhIP, Carcinogenesis 13 (1992) 629–635.
[23] J.C. Shen, W.M. Rideout 3rd, P.A. Jones, The rate of hydrolytic deamination of 5-methylcytosine in double-stranded DNA, Nucleic Acids Res. 22 (1994) 972–976.
[24] P.F. Swann, Why do O6-alkylguanine and O4-alkylthymine miscode? The relationship between the structure of DNA containing O6-alkylguanine and

O4-alkylthymine and the mutagenic properties of these bases, Mutat. Res. 233 (1990) 81–94.
[25] J.E. Goodman, L.J. Hofseth, S.P. Hussain, C.C. Harris, Nitric oxide and p53 in cancer-prone chronic inflammation and oxyradical overload disease, Environ. Mol. Mutagen. 44 (2004) 3–9.
[26] S. Djiogue, A.H. Nwabo Kamdje, L. Vecchio, M.J. Kipanyula, M. Farahna, Y. Aldebasi, P.F. Seke Etet, Insulin resistance and cancer: the role of insulin and IGFs, Endocr. Relat. Cancer 20 (2013) R1–R17.
[27] W. Li, Q. Ma, J. Liu, L. Han, G. Ma, H. Liu, T. Shan, K. Xie, E. Wu, Hyperglycemia as a mechanism of pancreatic cancer metastasis, Front. Biosci. 17 (2012) 1761–1774.
[28] P. Piątkiewicz, A. Czech, Głucose metabolism disorders and the risk of cancer, Arch. Immunol. Ther. Exp. (Warsz) 59 (2011) 215–230.
[29] T. Miyazawa, K. Nakagawa, S. Shimasaki, R. Nagai, Lipid glycation and protein glycation in diabetes and atherosclerosis, Amino Acids 42 (2012) 1163–1170.

Cancer and Inflammation Mechanisms

Chemical, Biological, and Clinical Aspects

Edited by

Yusuke Hiraku, Shosuke Kawanishi, Hiroshi Ohshima

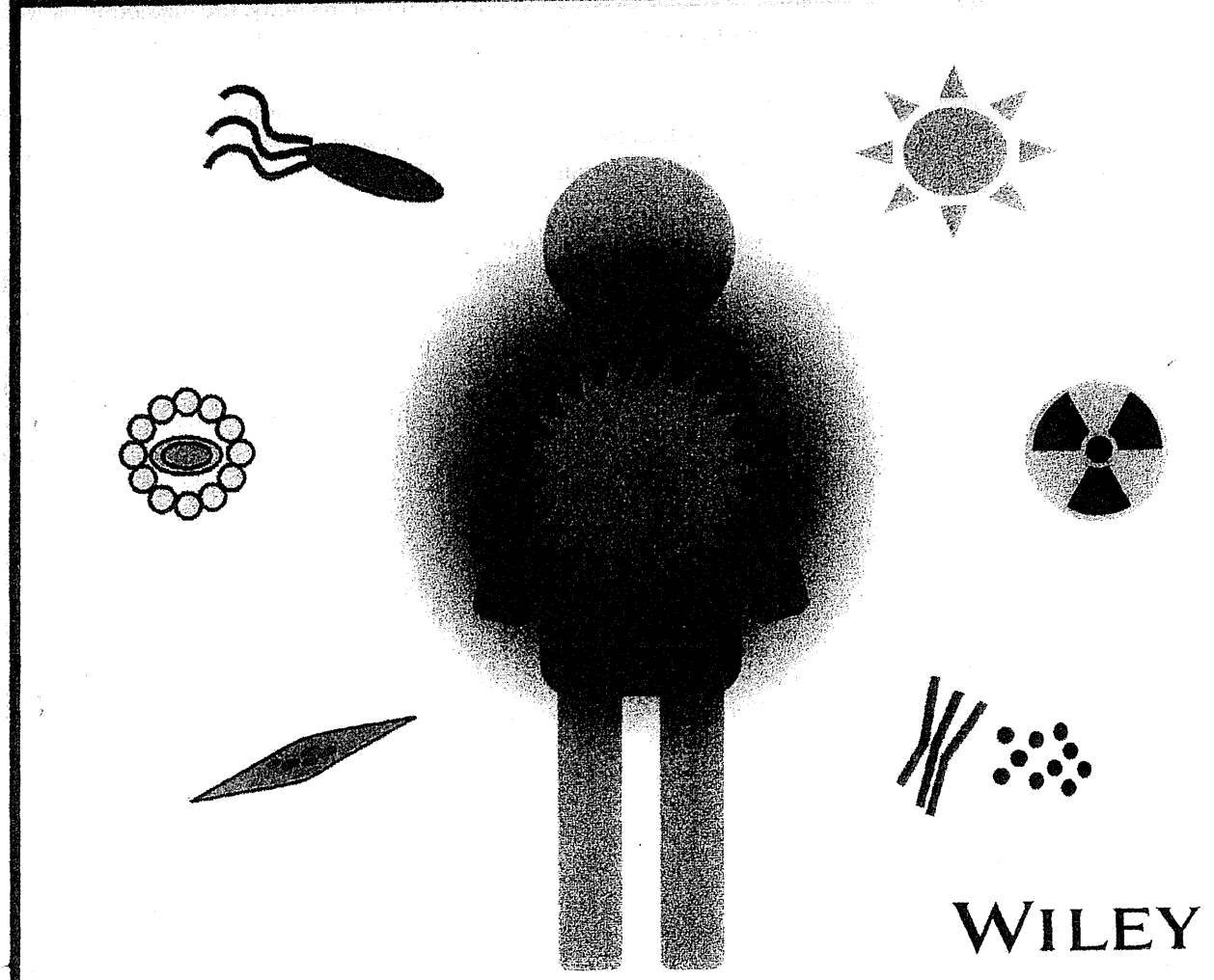

WILEY